

Research article

Open Access

A homotropic two-state model and auto-antagonism

Niels Bindslev*

Address: Department of Medical Physiology, Panum Institute, Blegdamsvej 3, DK-2200 Copenhagen N, Denmark

Email: Niels Bindslev* - bindslev@mfi.ku.dk

* Corresponding author

Published: 16 July 2004

Received: 02 December 2003

BMC Pharmacology 2004, 4:11 doi:10.1186/1471-2210-4-11

Accepted: 16 July 2004

This article is available from: <http://www.biomedcentral.com/1471-2210/4/11>

© 2004 Bindslev; licensee BioMed Central Ltd. This is an Open Access article: verbatim copying and redistribution of this article are permitted in all media for any purpose, provided this notice is preserved along with the article's original URL.

Abstract

Background: Bell-shaped and terraced dose-response relations have been observed in single ligand application for enzymes, carriers, transporters, G protein-coupled receptors as well as for other receptive units. It seems that there is still a need for new models as analytical tools for such dose-responses, especially in the light of expanding di- and multi-merization of the receptive units for functionality.

Results: Self-inhibition by drugs is analyzed in the frame-work of a theoretical homotropic two-state model, HOTSM. The model is a cubic reaction scheme based on a combination of conformational isomerization between two states within a receptive unit and ternary-complexing of two identical agonist molecules with the receptor. Concepts and terms related to self-inhibition are presented. HOTSM has seven independent parameters. Making a few simplifying assumptions narrows its analysis to initially look at four parameters. Some conclusions to be drawn are that a *first level* of spontaneous activity is solely determined by an isomerization constant, L . As ligand concentration rises, all seven parameters influence a *second level* of activity. At high ligand concentrations, a *third level* of activity is determined by only four of the seven constants, viz. the L constant and three intrinsic efficacy related constants, a , b , and d . The third level is given by $1/[1 + 1/(L \cdot a \cdot b \cdot d)]$. The third level may be above, at, or below the first and second levels. When the third level is above the first level, dose-responses may be bell-shaped, terraced, or reversed bell-shaped while when it is below the first level, dose-responses can attain forms of bell-shapes, reverse terraces, or reverse bell-shapes. To exemplify its use, the HOTSM is fitted to experimental dose-responses from sources in the literature. Development of the HOTSM is reviewed.

Conclusions: The homotropic two-state model, HOTSM, is a novel model for analyses of dose-responses at equilibrium that are co-operative or show bell-shapes of auto-antagonism.

Background

Agonists, inverse agonists, and antagonists all bind in a competitive fashion to primary binding sites in receptive complexes and thereby affect the function of receptors. The function of and binding to receptors and enzymes may further be modulated by allosteric compounds [1-6]. Such modulators, conventionally termed "effectors" in enzymology, bind to sites sterically separate from the pri-

mary binding site. Thus, the effect of binding a modulator molecule resembles non-competitive kinetics.

Regulatory modulation of receptor and enzyme function may be divided into heterotropic and homotropic allosteric behavior as originally defined by Monod and co-workers [7]. *Heterotropic allostery* is seen when an effect of a bound agonist or an enzymatic conversion of substrate

to product is altered by the binding of a different modulator molecule, eventually a product molecule, to a site different from the primary binding site on the receptive unit or the enzyme complex. *Homotropic allostery*, on the other hand, is seen when the agonist or the substrate itself binds to a modulator site and thereby affects the function of receptors or enzymes. This latter type of allosteric behavior is characterized as co-operative, and as such the term "co-operative" is used here in its strict sense only related to auto-modulation [5,8]. Dose-response relations with bell-shapes and terraces have been observed in single ligand applications both for enzymes [9,10], channel-, pump-, and co-transporters [11-14], carriers [15], tyrosine kinase receptors [16,17], and G protein-coupled receptors, GPCRs, for neurotransmitters, hormones, and chemokines [18-25].

Some recent examples of treatment by model of bell-shaped dose-responses have been carried out for receptive units in general [26], for monomeric enzymes [27], for growth hormone receptors [28], and for aggregation in antigen-antibody interactions [29].

With the realization of widespread dimer and multimer formation in functional units, including GPCRs [30], and the recognition of additional allosteric sites in these receptive unit [3,31,32] as well as for ABC transporters [33] and many others, it seems that there is still a need for mechanistic models where primary ligands (agonists) can operate as auto-modulators of function and simulate dose-response relations that display self-modulation in the form of either terraced curves or bell-shaped relations. One such model is the homotropic two-state model, HOTSM, presented here.

The HOTSM, which is a cubic ternary-complex reaction scheme, should be distinguished from two other recently developed cubic ternary-complex models. Thus, Hall has advanced a cubic ternary-complex reaction scheme with a receptor, an agonist, and a heterotropic modulator molecule in the form of an allosteric two-state model, ATSM [34]. This model is well-suited for analyzing dose-response data when the concentration of either the agonist or the modulator are varied separately. Another cubic ternary-complex reaction scheme developed for signal transduction in G protein coupled receptors, the so-called cubic ternary-complex model, CTCM, has been thoroughly analyzed by Weiss et al [35-37]. For the CTCM it is exclusively the activated and G protein-coupled receptor conformations that participate in the measured response.

Both agonism and agonist modulation appear simultaneously as the agonist concentration is varied in the HOTSM. Indeed, the HOTSM may describe self-modulatory phenomena of bell-shape, reverse bell-shape, terraces

and reverse terraces found in dose-response relations. The HOTSM appears as an appropriate reaction scheme in the analysis of dose-response relations for functional dimers as well as for other multimeric systems with a single type of ligand present. A historical development leading to the HOTSM is placed in **Appendix**

Concepts and developed terms

Concentration-dependent auto-antagonism and time-dependent desensitization

When a self-inhibitory dose-response relation is considered from an aspect of its dependence on the CONCENTRATION of a primary agonist or substrate, we may refer to such type of self-inhibitory phenomena as *auto-antagonism* or *negative co-operativity*. Alternatively, when the TIME-dependent aspect of self-inhibitory reaction kinetics is at center stage, we speak about *desensitization* or *inactivation*. Auto-antagonism due to increasing ligand concentration is by definition the same as negative co-operativity, since the term "co-operative", here, is solely used for homotropic allostery [5,8]. Meanwhile, "negative co-operativity" is related to shallow hyperbolic dose-response curves and usually does not cover bell-shaped dose-responses of auto-antagonism.

Results

The homotropic two-state model, HOTSM

In order to avoid misunderstandings, note that the term "two-state" refers to states of an unliganded receptive unit, and not to all possible receptor conformations.

HOTSM. Its analysis and evaluation

Fig 1 shows the equilibrium reaction scheme for homotropic allostery including two ligand binding sites, identified by the position on either side of the receptor symbol R, with possible different affinities, A_S and A_M , as well as unique intrinsic efficacy constants a and b for a bound agonist at either site, and further encompassing a two-state mechanism for activation of the receptive system, either in form of a 7-TM/tyrosine kinase receptor entity, an enzyme with prosthetic groups and co-factors, or a transport unit with several subunits, such as ion channels and pumps.

The symbols and parameters for the HOTSM reaction scheme in Fig 1 are listed below:

S = agonist or substrate and its concentration

R; RS; SR; SRS; and R*; R*S; SR*; and SR*S = concentration of various receptor conformations. "R" symbols with an "*" indicate active conformations, while "R" symbols without an "*" are receptive units in a quiescent state.

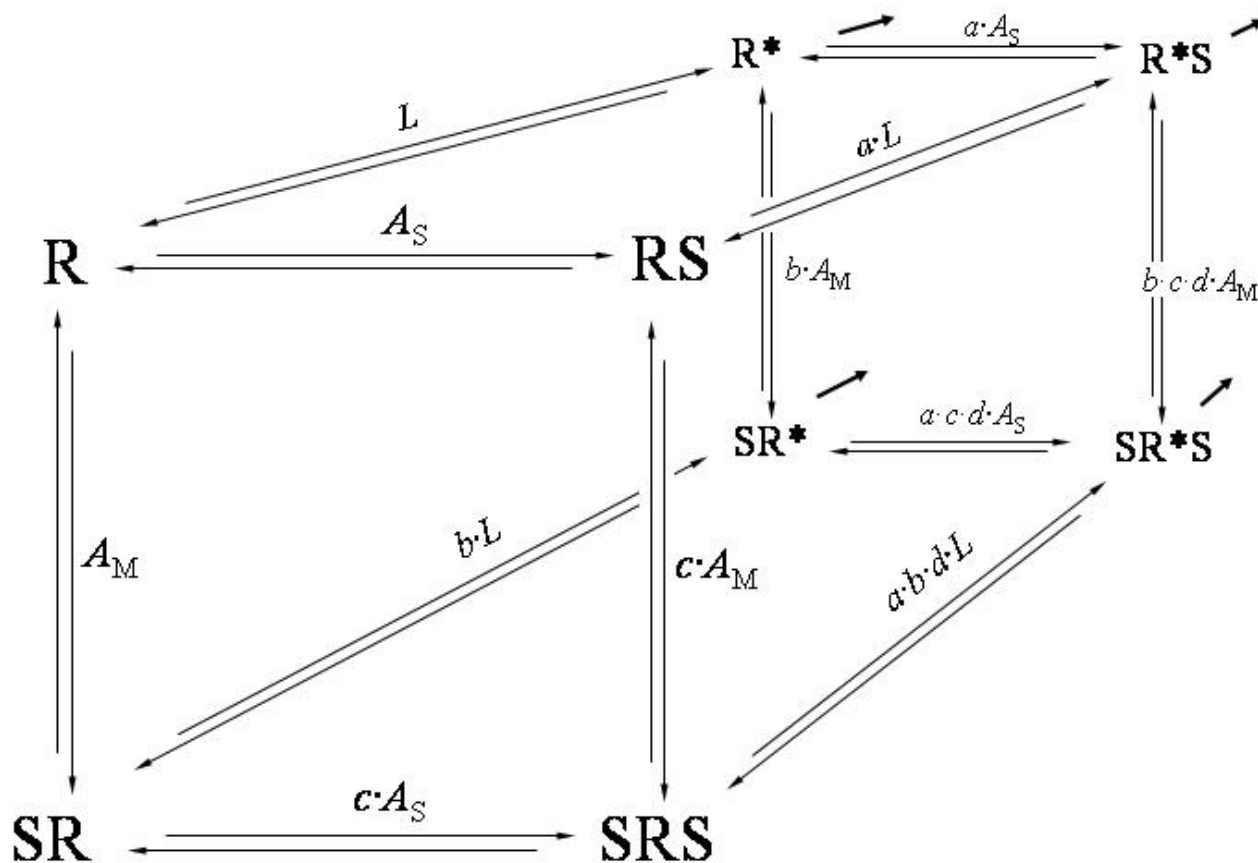


Figure 1

Reaction scheme for the homotropic two-state model, HOTSM. R is a receptive entity and S is a ligand, that can bind to two sterically separate sites in R. This is signified by positioning at either side of symbol R. The receptive unit in the unliganded condition exists in two conformations, a reactive form R and an active form R*. Arrows pointing into the plane of paper indicate the flow direction of signal transduction. There are 7 equilibrium constants in the HOTSM reaction scheme. All symbols are explained in the text.

L = the isomerization constant between unbound R^* and R, equal to R^*/R

A_S = the equilibrium association constant for S at the orthosteric site of R

A_M = the equilibrium association constant for S at the allosteric site of R

a = intrinsic efficacy for $R \rightleftharpoons R^*$ when S is already bound to the orthosteric site

b = intrinsic efficacy for $R \rightleftharpoons R^*$ when S is already bound to the allosteric site

c = co-operativity coefficient for S on binding to liganded R at either site

d = co-operativity coefficient for one ligand to be bound when another ligand is already bound to R^* 's or an intrinsic efficacy constant when two ligands are bound.

All seven system constants from L to d are forward constants. This choice was made to make it easier to appreciate the function of each parameter as the analysis

develops. Meanwhile, note that the efficacy-, co-operativity-, and isomerization constants are neither microscopic nor macroscopic [cf. [34]], and that the present isomerization constant L is reciprocal to the isomerization constant given for the original allosteric model, where the allosteric constant L was equal to R/R^* [7], or in their terminology T_0/R_0 .

Active receptor conformations in the HOTSM are depicted in Fig 1, and their fractional dose-response equation is given by

$$\frac{activity}{total} = \frac{R^* + R^*S + SR^* + SR^*S}{R^* + R^*S + SR^* + SR^*S + R + RS + SR + SRS} \quad (1).$$

This may be reformulated to

$$\frac{L \cdot (1 + b \cdot A_M \cdot S + a \cdot A_S \cdot S \cdot (1 + b \cdot c \cdot d \cdot A_M \cdot S))}{1 + A_M \cdot S + A_S \cdot S \cdot (1 + c \cdot A_M \cdot S) + L \cdot (1 + b \cdot A_M \cdot S + a \cdot A_S \cdot S \cdot (1 + b \cdot c \cdot d \cdot A_M \cdot S))} \quad (2)$$

or in a simplified form

$$\frac{active}{total} = \frac{x}{y + x} \quad \text{Functional - HOTSM,}$$

where $x = L \cdot (1 + b \cdot A_M \cdot S + a \cdot A_S \cdot S \cdot (1 + b \cdot c \cdot d \cdot A_M \cdot S))$

and $y = 1 + A_M \cdot S + A_S \cdot S \cdot (1 + c \cdot A_M \cdot S)$.

The saturation-variant of the fractional occupation relation for HOTSM is given by

$$\frac{saturation}{total} = \frac{x'}{x + y} \quad \text{Binding - HOTSM} \quad (3),$$

where $x' = x - L + y - 1$.

I shall first deal with an analysis of the functional HOTSM.

Functional-HOTSM. General considerations

Three plateaus of the functional-HOTSM

In the HOTSM, there are three levels of activated receptor conformations, Fig 2.

A basic level, which we may call the "first plateau", FP, is that of spontaneously active receptor conformations, R^* , before any ligand is added. In absence of ligands, the fraction of activated receptors is equal to $FP = R^*/[R+R^*] = L/[1+L] = 1/[1+1/(L)]$, and thus independent of all parameters except for L .

A second level of activity is found in the mid range of ligand concentrations, where ligands associate with the two binding sites to form in particular R^*S and SR^* . The form

and height of this second plateau, SP, and its position on the concentration axis all depend on the values of the seven independent parameters describing HOTSM.

A third level appears at high ligand concentrations, when ligands are bound to both primary and allosteric sites, maximizing the SRS and SR^*S receptor conformations. The level of response at the third plateau, TP, is only dependent on four of the system constants, viz. a , b , d , and the isomerization constant L , and is thus independent of parameters A_S , A_M , and c . The third plateau is given by $1/[1+1/(L \cdot a \cdot b \cdot d)]$.

From the expressions for the first and third plateau, it is easily deduced that TP is above FP for $a \cdot b \cdot d > 1$ and below for $a \cdot b \cdot d < 1$.

Bell-shapes, terraces, and co-operativities

It turns out that there are three features of the system activity to be analyzed in response to varying the values of the seven system constants, Fig 2. These three features are:

1) *bell-shaped dose-responses with maxima and minima*. We may ask, when does the HOTSM elicit a bell-shaped dose-response with an activity lower than maximum at higher concentrations of ligand. Which constants determine such behavior and which values for the constants are required? And furthermore, when reverse bell-shaped behavior with a minimum is observed, what are the values of relevant parameters?

2) *terraced and reversed terraced dose-responses*. The question is, which parameters are essentially involved when HOTSM yields either increasing or decreasing terraced dose-responses? And, which values are required for these parameters?

3) *co-operativity - positive or negative*. For co-operativity, without a bell-shaped dose-response relation, it is logical to ascertain which values of relevant parameters make the dose-response curve of HOTSM deviate from hyperbolic dose-response curves operative for simple one-sited systems.

Before a more detailed analysis of varying a single or a few parameters, the principal shapes that the dose-response curve of HOTSM can attain, as it possesses three plateaus, are demonstrated in figure 2 and listed here. The first and third response plateaus are locked with parameters L , a , b , and d . The position of the second plateau is further determined by parameters c , A_S , and A_M , and this plateau may a) be above the two other plateaus forming bell-shapes, b) be in between FP and TP yielding terraced or reverse terraced dose-responses, or c) be below both the other two plateaus and result in reverse bell-shaped dose-responses,

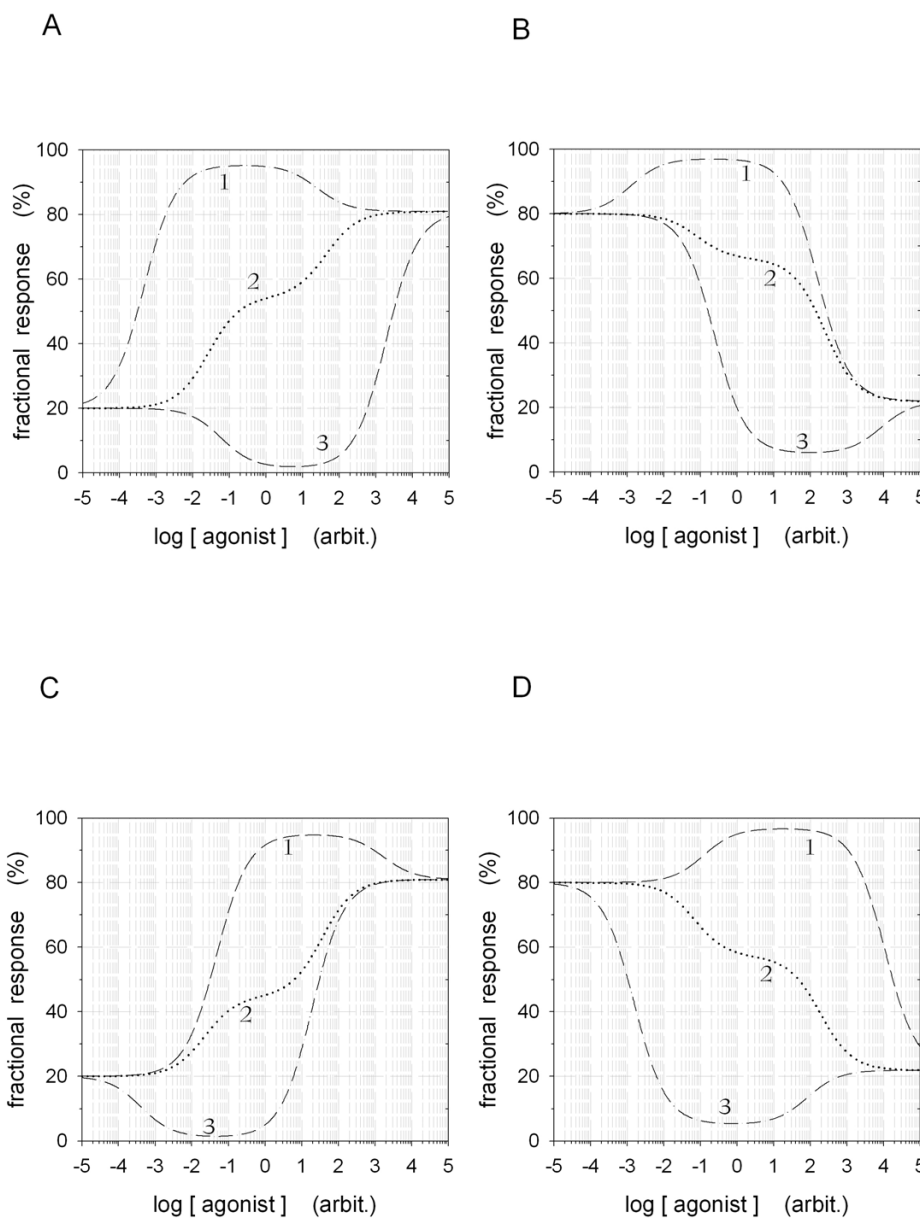


Figure 2

The response level of the functional-HOTSM has three plateaus. A first response-plateau, FP, in the absence of ligands is equal to $1/[1 + 1/L]$. A third response-plateau, TP, at high agonist concentrations is given by $1/[1 + 1/(L \cdot a \cdot b \cdot d)]$. Finally, a second-response plateau, SP, at intermediate ligand concentrations is dependent on all 7 parameters. The three plateaus may be above, at, or below each other, panels A-D, rendering dose-response curves that are positive or negative co-operative, bell-shaped or terraced, as well as reverse bell-shaped or reverse terraced. Parameter values in panels A-D were arbitrarily chosen in order to demonstrate several aspects of the model. A_S varied in three steps from 10^{-2} (-----) to 10^2 (-·-·-·-) by a factor 100 in panels A and B, while A_M varied in three steps from 0.3 (-----) to 3000 (-·-·-·-) by a factor 100 in panels C and D. The remaining parameters were fixed. Thus in panel A: $L = 1/4$, $A_M = 20$, $a = 100$, $b = 0.01$, $c = 0.01$, and $d = 17$. In panel B: $L = 4$, $A_M = 20$, $a = 10$, $b = 0.01$, $c = 0.01$, and $d = 0.7$. In panel C: $L = 1/4$, $A_S = 1$, $a = 100$, $b = 0.01$, $c = 0.01$, and $d = 17$. And in panel D: $L = 4$, $A_S = 1$, $a = 10$, $b = 0.01$, $c = 0.01$, and $d = 0.7$.

Fig 2. The second plateau may even disappear when values for c are above unity, and this will render increasing or decreasing mono-phasic dose-response curves, displaying negative or positive co-operativity as demonstrated later.

Simplifying constraints

Initial constraints

In analysis of HOTSM, the ratio between unbound receptive molecules in active and reactive states, $R^*/R = L$, is assumed to be at a low value of $1/30$. Thus, the analysis of HOTSM is simplified by choosing L to be fixed at $1/30$, meaning that the system operates at a 3% spontaneous activity.

Furthermore, in order to look at the system with a reasonably high response, initially I choose parameter a , as the intrinsic efficacy on ligand binding at the orthosteric binding sites, to be well above unity, $a \gg 1$, although, due to symmetry of the model, values for the intrinsic efficacy constants b and a may be interchanged without affecting the response curve, indicating that the concepts of the ligand as either primary ligand or modulator molecule can be switched freely. Finally, as the co-operativity parameter c does not change the level of either the first or third plateau of response, this parameter is initially kept less than one, $c < 1$. With these initial conditions the analysis narrows down to look for effects of variations in A_S , A_M , b , and d , and how they affect the characteristics of the system activity. This analysis is followed by a look at effects of varying c , L , and a .

Varying a single or a few of the parameters

Examples of varying constant b

Fig 3 shows the effect on the dose-response curve of varying the intrinsic efficacy constant for ligands at the modulator site, parameter b , in five steps with the other parameters fixed as indicated. The five values of constant b in panel A demonstrate how this parameter determines the second and third plateau of dose-response. With $b < 1$ and $A_S = A_M = 1$, for $b \cdot d < 0.5$ the dose-response curves are bell-shaped, and for $b \cdot d > 0.5$ they are terraced. When $a > b$, for $b \cdot d = 0.5$ the dose-responses are mono-phasic, cf Table 1. Fig 3 panel B is a 3-D illustration of separately varying the ligand concentration either at the orthosteric or at the modulator site for $b = 10$. Rising a plane along the response axis, following the arrow in the concentration plane of Fig 3B, will cut the 3-D topography and produce the 2-D curve in panel 3A for $b = 10$.

Examples of varying constant d

Fig 4 shows the effect of varying the co-operative affinity constant of active receptors/receptor double-liganded efficacy constant, parameter d , in five steps with the rest of independent constants kept fixed as indicated. Constant d , like b , also determines the second and third plateau of

the dose-response curve. In Panel A, since $a < b$, the dose-response curve is bell-shaped for $b \cdot d = 0.5$, cf Fig 3 and Table 1. Panel B in Fig 4 is a 3-D representation of the HOTSM function where the ligand concentration at the orthosteric and modulator sites are varied separately for $d = 0.005$. Rising a plane along the response axis, following the arrow in Fig 4B, will cut the 3-D topography and render the 2-D curve in panel 4A for $d = 0.005$.

As indicated in panels 3B and 4B, there are four plateaus in the 3-D topography of the HOTSM. One plateau is determined by parameter L ; of two other plateaus, one is mainly determined by parameter a and one by parameter b , while a fourth plateau is determined in particular by parameter d as well as by a , b , and L .

The 2-D and 3-D plots in Figs 3 and 4 illustrate the passage from a homotropic two-state model, HOTSM, with a single independent variable to an allosteric two-state model, ATSM [34], with two different ligand concentrations as independent variables, one for an agonist and another for a heterotropic modulator, cf *Comparison of HOTSM with ATSM* in the Discussion.

Examples of varying constant A_S

Fig 5 shows examples of the effect of varying the affinity constant for ligand binding at the primary site, A_S . In Fig 5A and 5B the affinity constant for ligand binding at the primary site, parameter A_S , is varied in five steps while the rest of the parameters are kept fixed as indicated, with $b < 1$. The third plateau of d-r curves goes from above the first and second plateau, as the product $a \cdot b \cdot d$ is kept above 1, panel A, to below, as the product $a \cdot b \cdot d$ is reduced below 1, panel B. The d-r curves, thus, display terraced, mono-phasic, bell-shaped, and reverse bell-shaped dose-response curves as A_S , b , and d varies. A situation where the third plateau is below plateau 1 but above plateau 2, is shown in Fig 2B curve 3. The criteria for panel B in Fig 5 can yield reverse terraced d-r curves, but this is more clearly demonstrated in Fig 2B curve 2, where the value of L is increased to 4.

Fig 5C and 5D shows d-r curves with the same variations of A_S as in panels A and B, but now keeping $b > 1$. The third plateau of dose-response curves decreases from above to below the first and second plateau, going from panel C to D by shifting the product $a \cdot b \cdot d$ from above 1, panels C, to below 1, panel D, resulting in terraced, mono-phasic, and bell-shaped curves.

A summary of the effects of combined variations in A_S together with b and d on the HOTSM dose-response curve is given in table 1.

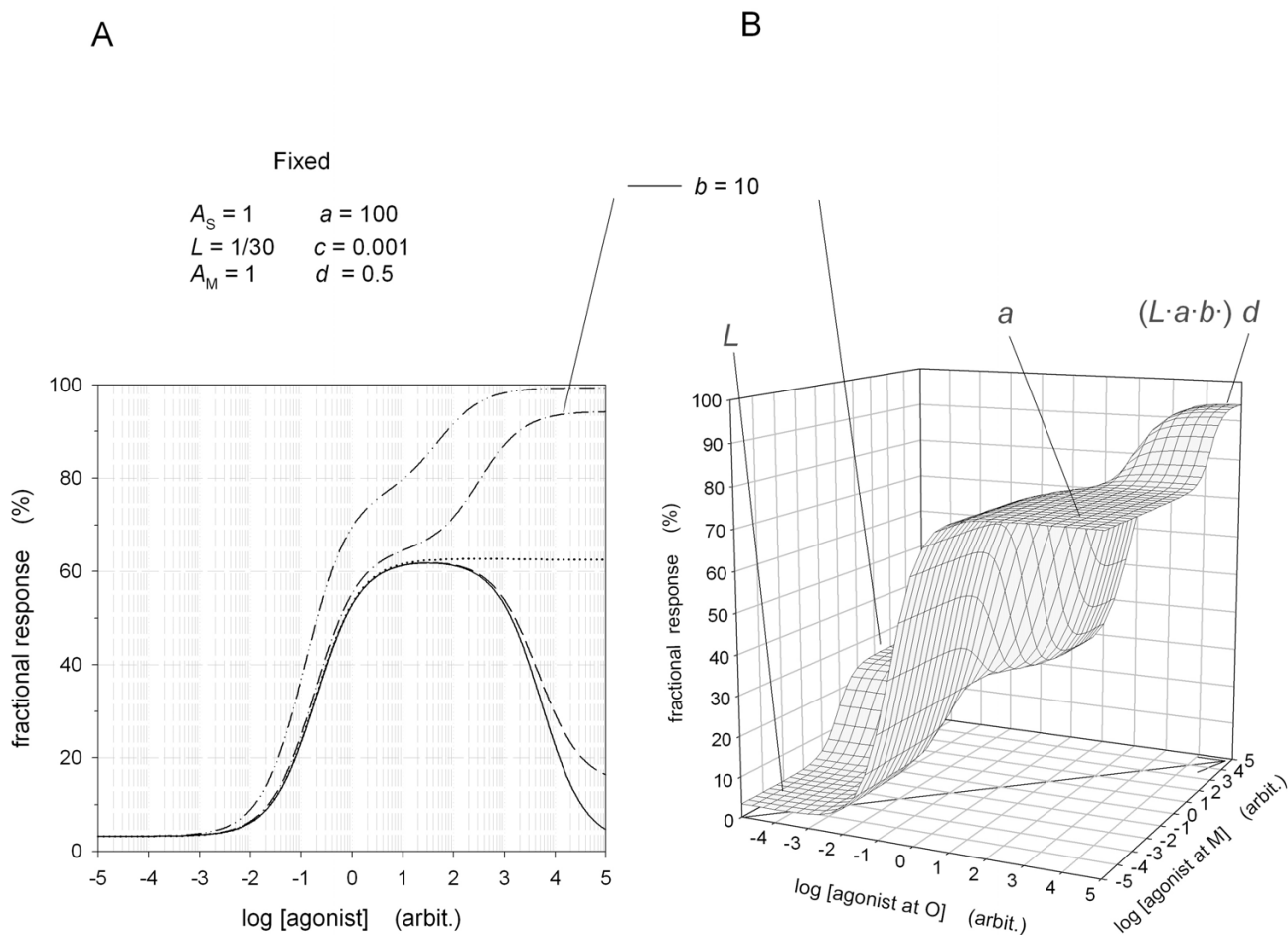


Figure 3
 Examples of varying parameter b for the functional-HOTSM dose-responses. Panel A, parameter b is varied in five steps increasing by a factor 10 from 10^{-2} (—) to 100 (---) with the other parameters fixed as indicated. Panel B is a 3 dimensional plot of separately changing the ligand concentration at either the orthosteric site, "O", the modulator site, "M", or simultaneously at both sites. Such 3-D plots are relevant for the switch from the HOTSM to the ATSM. Notice that $a = 100$ is above $b = 10$, and compare with figure 4B.

Table 1: Dose-response shapes for functional-HOTSM, when varying b , $b \cdot d$, and A_S . A_M , a , L , and c are fixed ($A_M = 1$, $a = 100$, $L = 1/30$, $c < 1$). With $A_S < 1$ at high agonist concentrations, the second HOTSM response level is below the start level when $b < 1$, Fig 5A and B, and above when $b > 1$, Fig 5C and D.

b	$b \cdot d$	$A_S > 1$	$A_S < 1$	Fig
< 1	> 1	terraced, mono-phasic	mono-phasic, reverse bell-shaped	5A
< 1	$= 1$	mono-phasic	mono-phasic, reverse bell-shaped	-
< 1	$= 0.5$	bell-shaped, mono-phasic	mono-phasic, reverse bell-shaped	-
< 1	< 0.5	bell-shaped	bell-shaped, mono-phasic, reverse bell-shaped	5B & Fig 2B
> 1	< 0.5	bell-shaped	bell-shaped, mono-phasic, terraced	5D
> 1	$= 0.5$	bell-shaped	bell-shaped \square , mono-phasic, terraced	-
> 1	$= 1$	mono-phasic, terraced	terraced	-
> 1	> 1	terraced	terraced	5C

\square For $a \gg b$ the bell-shape disappears and becomes mono-phasic.

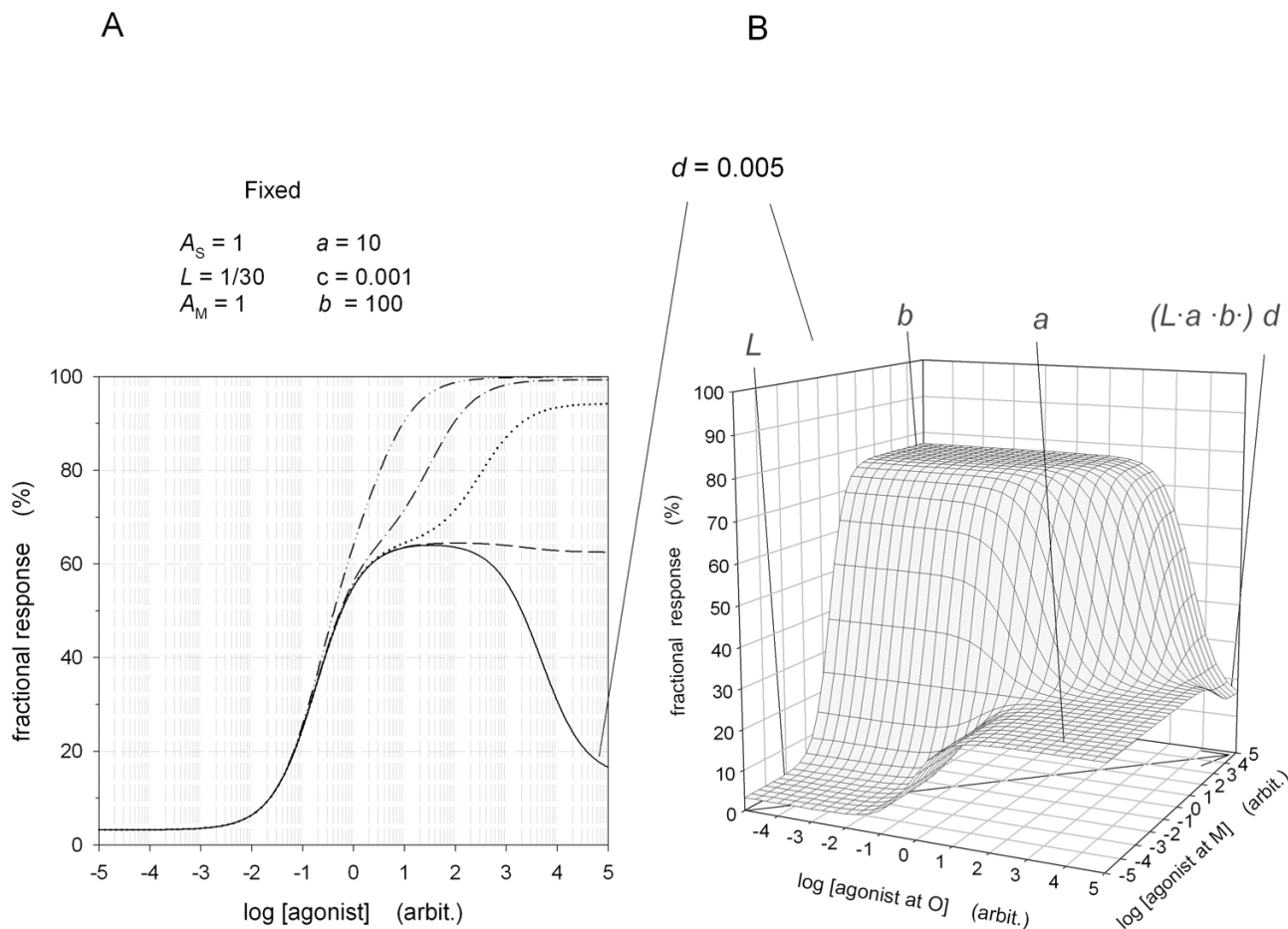


Figure 4
 Examples of varying parameter d for the functional-HOTSM dose-responses. Panel A, parameter d is varied in five steps increasing by a factor 10 from 5×10^{-3} (—) to 5×10^1 (-.-.-.-) with the other parameters fixed as indicated. Panel B is a 3 dimensional plot of separately changing the ligand concentration at either the orthosteric site, "O", the modulator site, "M", or simultaneously at both sites. Such 3-D plots are relevant for the switch from the HOTSM to the ATSM. Notice that $a = 10$ is below $b = 100$, and compare with figure 3B.

Examples of varying constant A_M

Fig 6 shows examples of the effect of varying the affinity constant for ligand binding at the modulator site, A_M . A_M is varied in five steps while the other independent parameters are kept fixed as indicated. In Fig 6A and 6B parameter b is <1 , while in panels C and D parameter b is >1 . In Fig 6, moving from panel A to B, the third plateau shifts from above the first and the second plateaus to being below these two plateaus. For large enough values of A_M , $A_M > 1000$, the HOTSM dose-response curves display inverse agonism in the low range of ligand concentrations. With the criteria in Fig 6A and 6B, we find terraced,

mono-phasic, bell-shaped and reverse bell-shaped dose-response curves. Slightly altering these criteria with A_M around 1 can also yield reverse terraced curves when the third plateau is below both the first and second plateaus, more clearly shown in Fig 2D, curve 2, varying A_M . With the conditions indicated for the dose-response curves in Fig 6 panels C and D, i.e. $b > 1$ as well as $a > 1$, there are no reversed bell-shapes or inverse agonism, no matter if the third plateau is above, at, or below the first and second plateaus. All the dose-response curves are either terraced, mono-phasic, or bell-shaped as A_M varies. A summary of

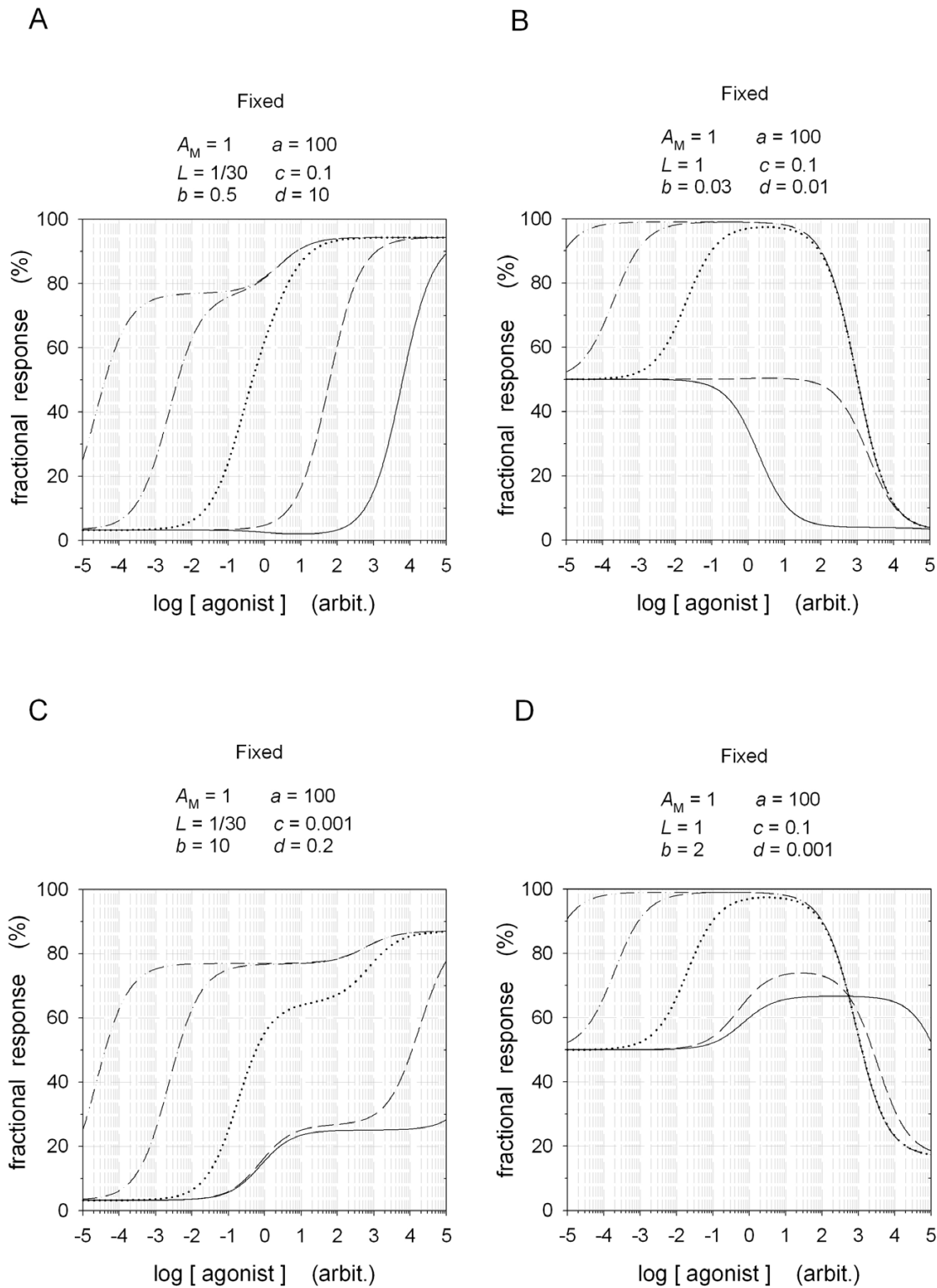


Figure 5
 Dose-response relationships for the functional-HOTSM varying parameter A_S in five steps from 10^{-4} (—) to 10^4 (-...-...) by a factor 100. Other parameters were varied as indicated. In panels A and B, b is less than unity, in panels C and D, b is above unity. The third plateau, $1/[1+1/(L \cdot a \cdot b \cdot d)]$, is above the first and second plateaus in A and C and below the first plateau in B and D. Thus, with conditions a and $b > 1$, the second plateau is always above the first plateau, panels B and D.

the effects on HOTSM dose-responses due to combined variations in A_M , b , and d are listed in table 2.

Considerations on A_S versus A_M

From the combined results of analyzing variations in A_S and A_M when $b < 1 < a$, as in panels A-B of Figs 5 and 6, there is "high-end inverse agonism" for $A_S \gg A_M$ and "low-end inverse agonism" for $A_S \ll A_M$, also demonstrated in Fig 2A,2B,2C,2D. Although not demonstrated, the converse is true for $a < 1 < b$ due to symmetry of the model.

Constant c

Analogous to how the affinity constants A_S and A_M affect the level of response at the second plateau and its position on the agonist concentration axis, c , a pure co-operativity factor of affinity, does influence the level of the second plateau in HOTSM and shifts its position and extension along the concentration axis. By increasing c above unity, it can eliminate the appearance of a second plateau.

Fig 7 shows examples of how the affinity constant c can separate the second and the third plateau of activity in HOTSM, without influencing the level of the first and third plateau. For $c < 1$ and with the third plateau above the first and second plateaus, i.e., $a \cdot b \cdot d > 1$, the HOTSM yields mono-phasic and terraced dose-response curves, Fig 7A. While, for c and b equal to or >1 plus $a > 1$, the second and third plateaus are layered on top of each other thus masking these two separate levels, Fig 7 panel A. Further, c , b , and $a > 1$ elicits the steepest dose-responses. These response curves may be analyzed for their positive co-operativity by fitting a four parameter Hill equation to generated response data. The conclusion of such an analysis is that the Hill coefficient reaches a maximum of 2 in the HOTSM, but as c is lowered, the Hill coefficient may drop below unity, Fig 7 panel A. In case the second level is in below the first and third level while the third level is below the first, we will observe mono-phasic or reverse bell-shaped curves, Fig 7B.

Variation in L

Parameter L is involved in the level of all three plateaus of the HOTSM dose-response curves, Figs 2 and 8. The higher the value of L the higher the level of all three plateaus. Since the first level of the dose-response is equal to the spontaneous level of activity for receptive units, parameter L also determines the size of possible inverse agonism, Fig 2. For use of the term "inverse agonism" see the comment on "inverse allosteric agonists" in section *HOTSM and inverse agonism* below. The first response plateau, solely determined by L , is not relevant for enzymes or transporters, since their activity is only measurable in the presence of ligands.

Constant a as intrinsic efficacy at the orthosteric site

So far in this analysis, constant a has been taken as the intrinsic efficacy for ligand binding at the primary binding site. When complexes R^*S and SR^* are equally active as indicated in Fig 1, then in a classic comprehension of the terms "orthosteric" (primary) and "allosteric" (secondary, modulator) sites, it is required for a to be larger than b , and A_S to be above A_M in order for a by definition to be the intrinsic efficacy constant and A_S the affinity constant for binding at orthosteric binding sites of the system. A bit more detailed: for $a > 1 > b$, a is the intrinsic efficacy at the orthosteric site no matter what the relation is between the two affinity constants A_S and A_M , while for $a > b > 1$, a is only the intrinsic efficacy constant at the orthosteric site if also $A_S > A_M$.

The manner in which a and b affect the HOTSM dose-response relation is further visualized in panels 3B and 4B. Here parameters a and b determine either of two plateaus when ligands interact separately with a primary site, "O", or a modulator site, "M", as for the allosteric two-state model, ATSM.

Other features of the HOTSM

Co-operativity – positive or negative – in HOTSM

As already mentioned, examples of negative and positive co-operativity are demonstrated for the HOTSM in Fig 7A. Employing the Hill coefficient from a Hill plot analysis on the generated dose-response curves as a measure of co-operativity, we can identify that positive co-operativity may be observed for the HOTSM increasing to Hill coefficients of 2, curve 1 Fig 7A, while negative co-operativity is observed as the Hill coefficient falls below unity, curve 2 Fig 7A, and may even drop to zero and negative values, B panels in Figs 5, 6, and 7.

Conditions for reverse bell-shaped responses

Conditions for when the HOTSM elicits reverse bell-shapes can be derived from the realization, that a first level of dose-response is below a third level when $a \cdot b \cdot d > 1$ and the other way around, that a first level of response is above a third level when $a \cdot b \cdot d < 1$.

Thus, for $a \cdot b \cdot d > 1$ there is reverse bell-shaped responses, curve 3 in Fig 2A and 2B, when

$$A_M + A_S + c \cdot A_M \cdot A_S \cdot [S] > b \cdot A_M + a \cdot A_S + a \cdot b \cdot d \cdot c \cdot A_M \cdot A_S \cdot [S]$$

and for $a \cdot b \cdot d < 1$ there is reverse bell-shaped responses, curve 3 in Fig 2C and 2D, when

$$(1 + A_M \cdot [S] + A_S \cdot [S]) \cdot a \cdot b \cdot d > 1 + b \cdot A_M \cdot [S] + a \cdot A_S \cdot [S].$$

It may be seen that all system parameters except L are involved in these conditions and that reverse bell-shapes

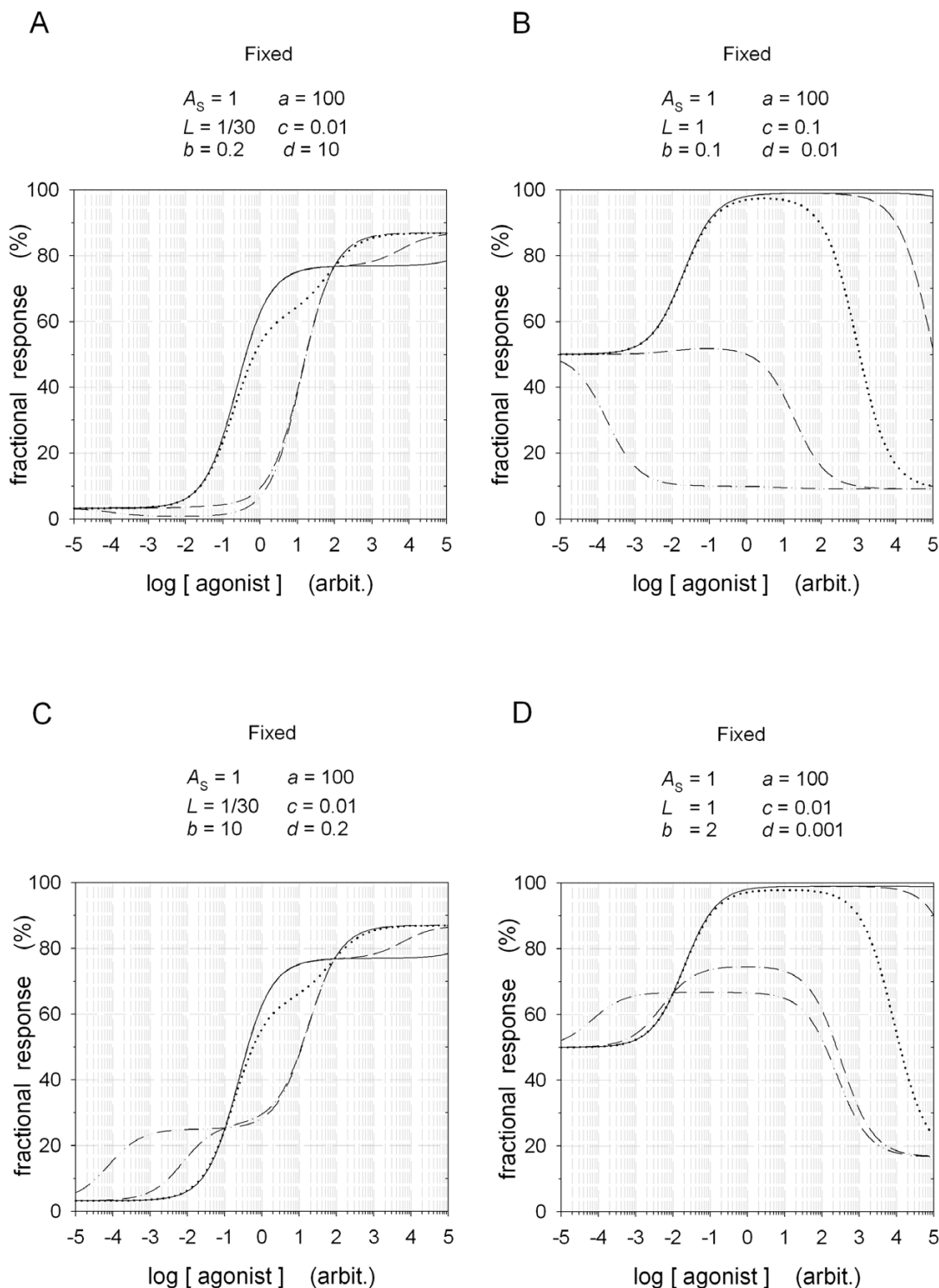


Figure 6

Dose-response relationships for the functional-HOTSM varying parameter A_M in five steps from 10^{-4} (—) to 10^4 (-.-.-.-) by a factor 100. Other parameters were varied as indicated. In panels A and B, $b < 1$, and in panels C and D, $b > 1$. The third plateau, $1/[1+1/(L \cdot a \cdot b \cdot d)]$, is above the first and second plateaus in panels A and C and below the first plateau in panels B and D. With conditions $b < 1$ and $TP > FP$, the HOTSM results in reverse bell-shaped dose-effect curves, panels A to C. For the conditions a and $b > 1$, the second plateau is always above the first plateau, panels B and D.

Table 2: Dose-response shapes for functional-HOTSM, when varying b , $b \cdot d$, and A_M . A_S , a , L , and c are fixed ($A_S = 1$, $a = 100$, $L = 1/30$, $c < 1$). With $A_M > 1$ at low agonist concentrations, the second HOTSM response level is below the start level when $b < 1$, Fig 6A and B, and above when $b > 1$, Fig 6C and D.

b	$b \cdot d$	$A_M > 1$	$A_M < 1$	Fig
< 1	≥ 1	reverse bell-shaped, mono-phasic, terraced	terraced	6A
< 1	$= 0.5$	reverse bell-shaped, mono-phasic, terraced, mono-phasic	mono-phasic, bell-shaped	-
< 1	< 0.5	reverse bell-shaped, mono-phasic, terraced, mono-phasic bell-shaped	bell-shaped	6B & Fig 2 D
> 1	≥ 1	terraced	terraced	6C
> 1	≤ 0.5	terraced, mono-phasic, bell-shaped	bell-shaped	6D

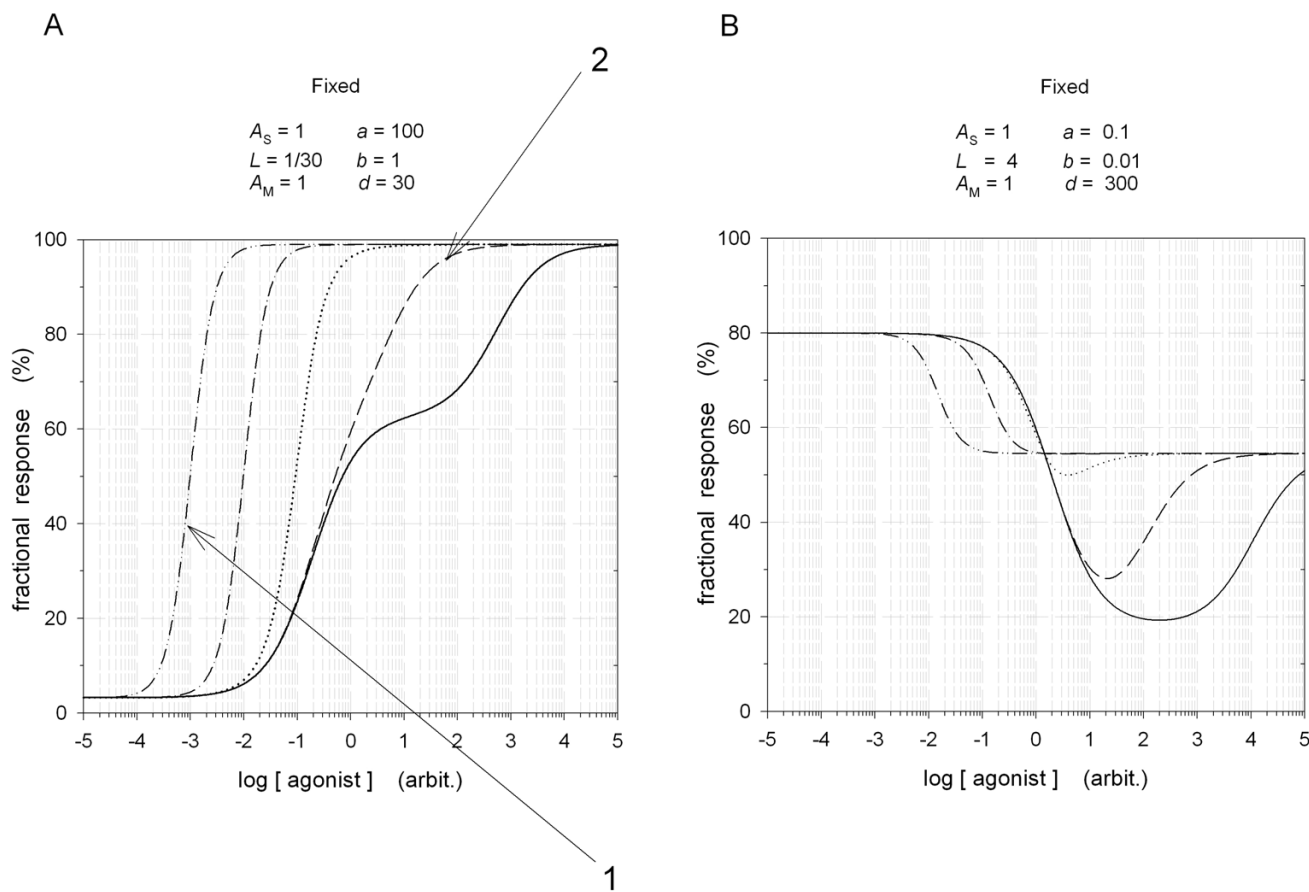


Figure 7

Dose-response relationships for the functional-HOTSM with focus on variation in c . Constant c is varied in five steps from 10^{-4} (—) to 10^4 (-.-.-.-) by a factor 100. Other parameters were varied as indicated. The third plateau at high concentrations, $1/[1+1/(L \cdot a \cdot b \cdot d)]$, is independent of parameter c . Parameter c determines the width of the second plateau, thus for decreasing values of c the width broadens. The third plateau, TP, is above the first and second plateaus in panel A. In panel B, TP is below the first plateau but above the second plateau, eliciting reverse bell-shaped curves for certain parameter values. Fitting a four parameter Hill equation to the steepest dose-response curve 1 in panel A yields a Hill coefficient, n_H , equal to 1.99, while a fit to the dose-response curve 2 in panel A give $n_H = 0.68$, for $c = 100$.

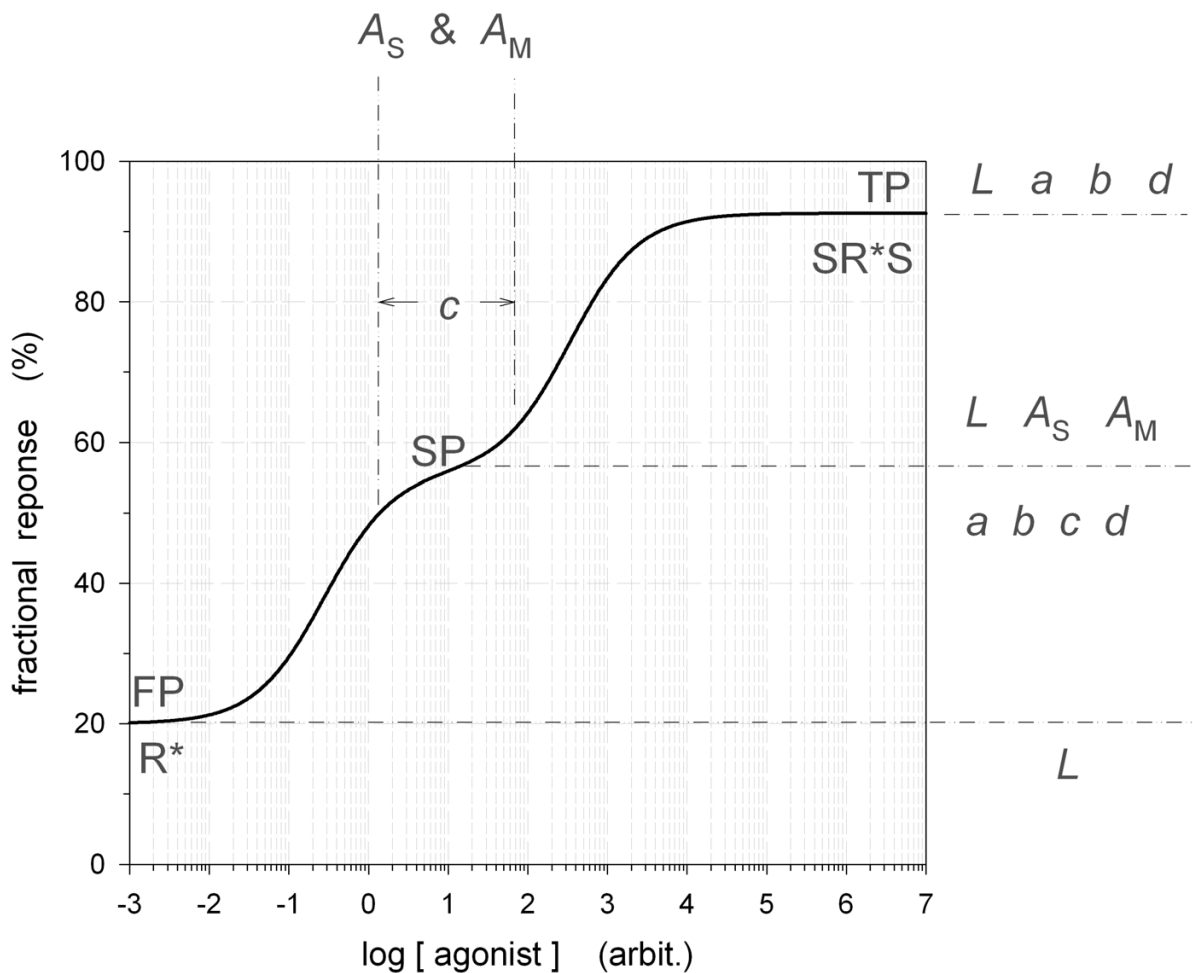


Figure 8

A principal drawing of the three plateaus for the functional-HOTSM. Parameters that determine each plateau are indicated to the right. The first plateau is determined by the fraction of R^* conformations in the absence of ligands. When maximal fractions of SRS and SR^*S are obtained at high ligand concentrations, the level of response is given by the four parameters a , b , d , and L , see Fig 1, and not dependent on either c , A_S , or A_M . The three latter parameters determine the width and the mid-point position at the concentration axis of the second plateau of response.

only appear for a given range of ligand concentrations. From these conditions it may also be derived that either a or b have to be <1 in order to observe reverse bell-shaped dose-responses.

The midpoint of the second plateau

The second plateau, SP, of the HOTSM dose-response curve is illustrated in Fig 8. The response level of the midpoint of this plateau is determined by all seven system constants as indicated in Figs 2 to 7. The effect of parameter c on the second plateau and its midpoint is only indirect, since c as demonstrated in Fig 7, only squeezes or

broadens this plateau along the agonist concentration axis. Thus for values of $c > 1$, as already stated, this second level may vanish completely. The position and extension of the second plateau on the agonist concentration axis is also determined by affinity parameters A_S and A_M , and like parameter c they do not alter the height of the second plateau. Increasing both A_S and A_M with an identical factor moves the midpoint of SP to the left on the agonist concentration axis with the same factor, while reducing both parameters with the same factor moves the midpoint to the right with an identical factor. These changes in A_S and A_M does not alter the extension of the second plateau. For

this to happen, the two affinity parameters must change values in opposite directions. Parameters a , b , d , and L does not affect the position of the midpoint for the second plateau on the agonist concentration axis.

Application of HOTSMS to experimental data

The usefulness of the HOTSMS as a tool for mechanistic interpretation of experimental dose-response data is illustrated here in a preliminary fashion by fitting the model parameters to examples from the literature. In the analysis a few simplifying constraints on the parameters are implemented. Thus, in all the examples $a = b$ and in the exam-

ples with convex bell-shaped dose-response curves, A_S is kept equal to A_M as well. These assumptions simplify the parameter fitting and are justified for receptive units supposed to consist of homo-dimers. Values for parameter L and factor $L \cdot a \cdot b \cdot d$ are determined from estimates of the basal and third level of activity and used in the analyses.

1) We found a dramatic auto-antagonism for acetylcholine when stimulating exocrine secretion in tracheal epithelium [18]. Fitting the HOTSMS to data from this study is presented in Fig 9A for L fixed at 1/100. Obtained parameter values are in the figure legend.

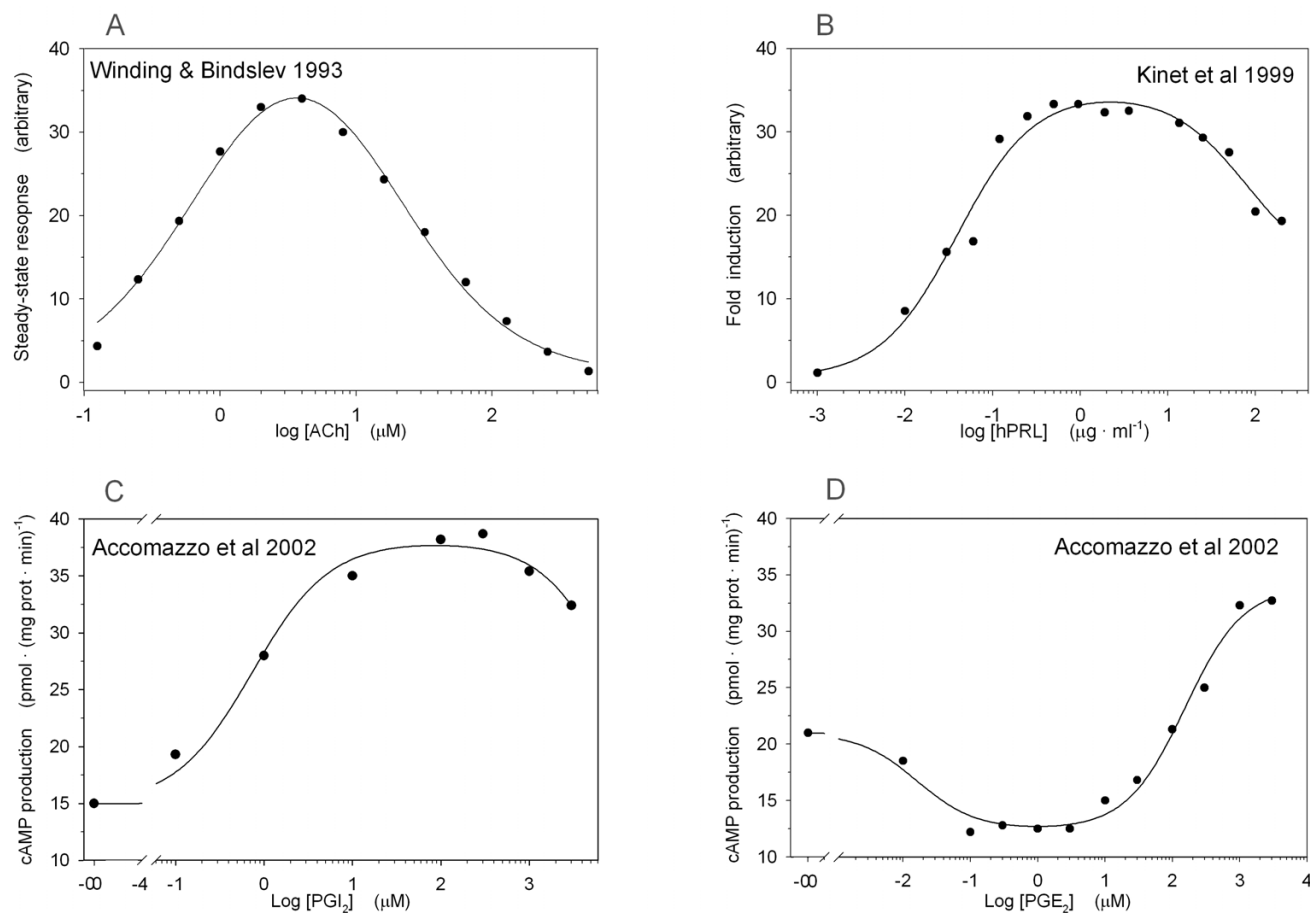


Figure 9

Examples of fitting HOTSMS to experimental data sets taken from indicated sources. The general constraints for fitting is that all seven parameters are positive and $a = b$. Panel A: additional conditions for a fit to the data set of Winding & Bindslev [18] are: $L = 1/100$ and $A_S = A_M$; which yields $a = b = 93.7 \pm 11.8$, $c = 0.677 \pm 0.295$, $d = 1.05 \pm 1.18 \cdot 10^{-4}$, and $A_S = A_M = 0.329 \pm 0.069$. Panel B: additional conditions for a fit to the Kinet et al [38] data are: $L = 1/100$ and $A_S = A_M$; yielding $a = b = 54.2 \pm 2.7$, $c = 5.03 \pm 3.25 \cdot 10^{-3}$, $d = 5.20 \pm 2.11 \cdot 10^{-3}$, and $A_S = A_M = 7.81 \pm 1.39$. Panel C: the convex bell-shaped data set of Accomazzo et al [Fig 1A in 39] has the following conditions added to the general constraints: $L = 0.1765$ and $A_S = A_M$; yielding $a = b = 3.48 \pm 0.16$, $c = 3.79 \cdot 10^{-4} \pm 2.202 \cdot 10^{-3}$, $d = 0.634 \pm 0.633$, and $A_S = A_M = 0.496 \pm 0.129$. Panel D: the reverse bell-shaped data set from Accomazzo et al [Fig 1D in 39] has the following conditions added to the general constraints: $L = 0.2658$, $a \cdot b \cdot d = 1.938$, $A_S < 1$, and $A_M > 1$. The obtained fitted parameters are: $a = b = 0.532 \pm 0.030$, $c = 0.337 \pm 0.176$, $A_S = 1.47 \pm 0.79 \cdot 10^{-2}$, and $A_M = 68.3 \pm 36.2$. From the fitted value for a and b , parameter d may be calculated: $d = 1.938/(0.532)^2 = 6.85$.

2) Kinet et al [38] measured transcriptional induction by the prolactin hormone. A fit of the HOTSM to their experimental data is shown in Fig 9B, again with L fixed at $1/100$, and yields values for parameters as indicated in the figure legend.

3) A third and a fourth example are taken from Accomazzo et al [39], who presented both ordinary and reverse bell-shaped dose-responses for cAMP production by PGI₂ and PGE₂. Fits of the HOTSM to their data are presented in Figs 9C and 9D. Parameter L was estimated to 0.177 for the convex bell-shape of cAMP production with increasing PGI₂ concentration.

For the concave (reverse) bell-shaped dose-response curve in Fig 9D, parameter L was estimated to 0.266 and the factor $a \cdot b \cdot d$ to 1.94. In this example, parameters A_S and A_M were allowed to vary independently, an obligatory condition in order to get a fit to reverse bell-shapes when parameter a and b are kept equal. The HOTSM parameter estimates for these two example are also in the figure legend.

Estimates of factor $a \cdot b \cdot d$

To get good fits of the HOTSM to dose-response data, it is recommended, if possible, to operate within a narrow range of values for the product $a \cdot b \cdot d$. This product may be estimated from a combined determination of the initial level of response, which yields the value of parameter L , and of the third plateau, equal to $1/[1+1/(L \cdot a \cdot b \cdot d)]$. Thus, when bell-shaped or terraced d-r curves are obtained it may be worth analyzing the d-r relations at high enough concentrations of the ligand in order to get a good estimate of a third plateau. This is not the usual practice. When deviations from simple Langmuirian dose-responses appear, practice is to abrogate ligand application before a possible third plateau is reached.

Binding-HOTSM

Binding experiments

A formula describing the binding-variant of the HOTSM is given in equation 3. Due to the symmetry of the HOTSM, its concentration-binding curves are all mono-phasic increasing from 0 to 100%, with varying steepness, but without bell-shapes, terraces, or reverse ditto. Examples of the dose-binding relations varying the single parameters are shown in Fig 10. Table 3 is a summary of the effects on position and steepness of concentration-binding curves due to varying each of the seven parameters in the HOTSM reaction scheme for ligand binding. Displacing bound tracer ligand with its non-radioactive isotope will yield the same concentration-binding relations, just in reverse, as all parameters are the same. The HOTSM may thus be useful for an analysis of the steepness for frac-

tional binding in tracer concentration-saturation and -displacement experiments.

Terraced and bell-shaped concentration-displacement relations seen with heterotropic modulators, as found and analyzed with one-state equilibrium or kinetic models by for instance Wreggett & Wells [40] and Avlani et al [41], are relevant for the allosteric two-state model ATSM, but not for HOTSM. Meanwhile, the ATSM in its presented form for binding [34] does not cover bell-shaped or terraced concentration-displacement relations by heterotropic ligands.

Discussion

Themes related to the homotropic two-state model

Mechanistic interpretation of experimental data by HOTSM and Hill's equation

The HOTSM is a mechanistic model. In the theoretical presentation of the HOTSM, Fig 1, it is assumed that a single receptive unit possesses two binding sites that can interact on a graded scale, which is measurable as variation in parameters such as A_M , b , c , and d . Meanwhile, the interpretation of the HOTSM parameters will depend on the actual system under analysis.

Applying the HOTSM in an analysis of dose-response data from systems with G protein coupled receptors, these parameters may be relevant for steps down-stream from the receptor sites in the signal-transduction pathway. As an example, for mGluR dimers the parameters A_M , b , c , and d may pertain to conformational changes at the interface between the two receptor subunits [6].

Ordinary (convex) and reverse (concave) bell-shaped dose-response curves have often been analysed by a sum of two Hill equations [20,22,39]. However, these analyses have their limitations, since as a mechanistic description, Hill equations only cover for full simultaneity in occupancy, equal to an all-or-none co-operativity between binding sites or subunits. Therefore, development of new mechanistic models like the HOTSM seems warranted.

There are 6–7 system constants to be determined in both the HOTSM and the double-Hill equation. For the HOTSM, parameter L can often be estimated from the initial activity with no ligand present and the factor $L \cdot a \cdot b \cdot d$ from the activity at high concentrations of an agonist. Also the range of parameters c , A_S , and A_M may be estimated from the obtained dose-response curves. These estimates will simplify the least-square analysis for non-linear parameter fitting.

As presented here in its simplest form, the HOTSM is limited by its failure to describe steep dose-responses. Its maximal Hill coefficient is 2, Fig 7. Therefore to analyse

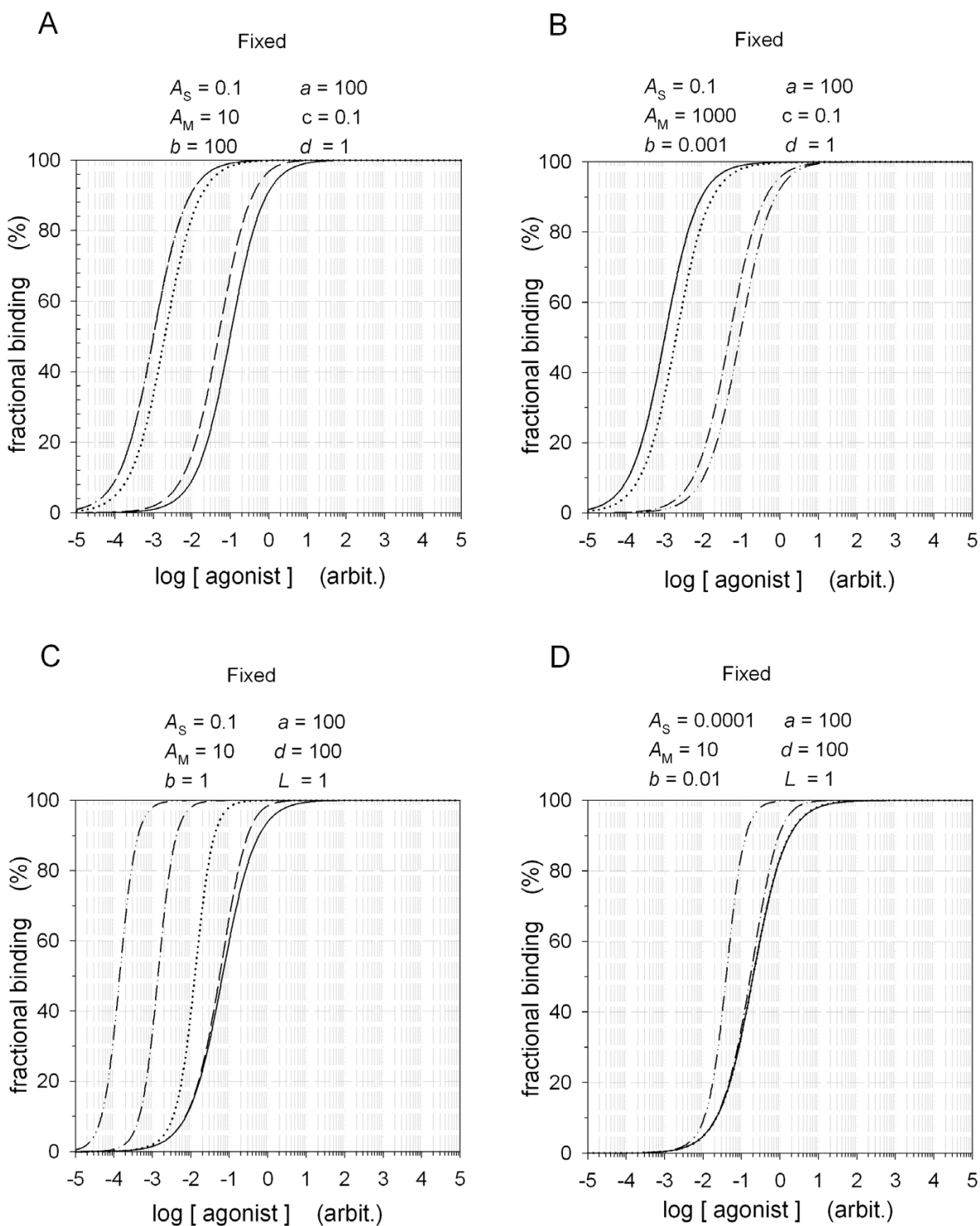


Figure 10

Examples of the concentration-binding relationships for HOTSMS when varying parameters L or c in five steps from 10^{-4} (—) to 10^4 (-.-.-) by a factor 100. Other parameters were varied as indicated. With $a > 1$ and increasing ligand concentrations, parameter L is the sole system constant that can move the concentration-binding curves for HOTSMS either to the left, for $b > 1$, panel A, or to the right, for $b < 1$, panel B. Examples of varying parameters c , b and A_S are shown in panels C and D. The effects of increasing parameter L , c and the other five parameter on the position and steepness of the concentration-binding curves for the HOTSMS are summarized in table 3.

Table 3: Effects on position and steepness of concentration-saturation relationships when varying single independent system constants. Parameter values were typically varied between 10⁻⁴ to 10⁴. Except for indicated variations in *a*, the table is collected for parameter *a* = 100.

increasing value of parameter	move mono-phasic dose-binding curves to	Hill coefficient of dose-binding curves may go from
<i>a</i>	left	<1 → ~1
<i>b</i>	left	<1 → ~1
<i>c</i>	left	1 → 2
<i>d</i>	left	<1 → ~1
<i>A_S</i>	left	1 → 2
<i>A_M</i>	left	1 → 2
<i>L</i> for <i>A_S</i> > 1	left	1 → 2
<i>L</i> for <i>A_S</i> & <i>b</i> < 1	right*	1, for <i>d</i> >> 1 1 → 2

* for *d* >>> 1 may go left

steep dose-response relationships, a further development of the HOTSMS will be necessary. On the contrary, although use of the Hill equation most often only yields a semi-quantitative estimate of co-operativity for the studied system, it is capable of fitting to steep accelerating dose-responses.

Interpretation of HOTSMS parameters based on experimental data
 In evaluation of parameters from theory adjusted to experimental data as exemplified in Fig 9, parameter *a* was kept equal to *b* and parameter *A_S* equal to *A_M*, except for the example in Fig 9D with reverse bell-shaped dose-response, where *A_S* and *A_M* were allowed to vary independently. These simplifying assumptions for two separate binding sites seem reasonable when dealing with receptive units likely to consist of homo-dimers.

Reverse bell-shaped dose-responses are discussed separately in a section below.

For the first example of fitting theory to experimental data, Fig 9A, a detailed interpretation of the parameter estimates involve a discussion of muscarinic receptors with a focus either on orthosteric and allosteric binding sites [31,32], on oligo/dimer interactions [42] as suggested in the original article, on bifurcation further down-stream in the signal-transduction pathway [43], or on regulatory changes as desensitization mechanisms that vary with ligand concentration, also discussed by Winding & Bindslev [18].

In the second data example from Kinet et al [38], interpretation of obtained parameters is most likely related to the dimerization of prolactin receptors upon activation [44] and an ensuing interaction at the interface between two receptor subunits. All seven HOTSMS constants may be

dependent on such an interaction. But, since conformational steps of importance for function in this system may be physically remote from the actual process of dimerization, differentiating between effects of dimerization and of functional conformation, based on the obtained parameter values, will require knowledge about states of activation for the dimer and the full chain of events in signaling.

In the two examples above, Fig 9A and 9B, where parameters *a* and *b* were found >1, the "negative" coupling is effectuated by parameter *d* << 1, sufficient to result in bell-shaped dose-responses. One interpretation of the low values for parameter *d* is a possible prevention of receptor activation when both binding sites are occupied, although an experimental verification of such a scenario has to be established. The value of *c*, which determines broadness of the bell, was much less than unity for the broadest bell-shape in the Kinet et al example and closer to unity for the Winding & Bindslev data. This is in accordance with the theoretical analysis evaluating the effects of varying a single parameter, see Results section on varying *c*, and indicates a tighter negative coupling between sites on binding for the example in Fig 9A.

In the two examples from Accomazzo et al's study [39], Fig 9C and 9D, it is possible to make an accurate estimate of the distribution between unliganded active and reactive (quiescent) receptor conformations. Thus *R^{*}/R* = *L* = 0.177 in the first example, Fig 9C, and = 0.266 in the second example, Fig 9D. Further, for the second data set in figure 9D a rough estimate of the factor *L · a · b · d* can be assessed, yielding 1.94 for *a · b · d* on a relative scale.

The obtained parameter estimates may be interpreted in the light of an interaction being either at the interface

between two simultaneously expressed receptors or at a step further down-stream in the signal chain, as assumed by the authors [39].

Experimental reverse bell-shaped dose-responses

Reverse bell-shaped dose-response relations are often seen when two GPCRs, coupled to different G proteins, are expressed simultaneously and actually rendered probable as a bifurcation due to coupling to different G proteins [22,23,39,43]. However, this is not an explanation for the reverse bell-shaped dose-response relation as seen in the Hornigold et al study, when expressing a single muscarinic receptor subtype, m3, in CHO cells [22]. Here dimerization of m3 receptors is a more likely explanation for bell-shaped dose-responses.

Therefore, in the second example by Accomazzo et al, with $a = b$ Fig 9D, a possible interpretation of the PGE₂-dependent reverse bell-shaped dose-response seems to be that, by dimerization of two PGE₂ subtype receptors, the affinities at the two binding sites are dramatically altered, as the fitted value of parameter A_M has to be nearly 5000 fold higher than A_S to accommodate theory to experimental data, Fig 9D. Meanwhile, intuitively this does not seem to be a correct explanation, although coupling to G proteins might induce such a differentiation between A_S and A_M .

A second possibility is instead to keep $A_S = A_M$ and let a and b float independently of each other. Meanwhile, it turns out that these conditions cannot accommodate the model to experimental data in Fig 9D, and neither to the m3 data in Hornigold et al [22], fitted results not shown.

Thus, in case the HOTSM is the right mechanistic model for PGE₂ effects on cAMP production in smooth muscle cells [39], and for methacholine effects on forskolin-induced cAMP generation [22], a third possibility might be an emergence of an alternative homotropic binding site in the receptive unit due to dimerization. Obviously, studies that can substantiate either of these interpretations – establishment of two non-identical binding sites upon dimerization or the appearance of a supplementary, homotropic allosteric site with or without dimerization – will be interesting to follow. One place to start could be the structure of functional m3 receptors in CHO cells as they result in reverse bell-shaped dose-responses, even when expressed as the sole receptor type [22].

Required reciprocity

The present analyses make explicit, that with the full reversibility in the models, they satisfy Colquhoun's justified demand for thermodynamic reciprocity in modeling the affinity and efficacy for binding and function [45]. This reciprocity also allows the primary binding site and

the modulator binding site to be conceived as fully symmetrical and interchangeable. Obviously, mathematical derivation of a fractional activity from a completely symmetric model does not differentiate between two such binding sites, and therefore, the behavior of the model yields completely symmetrical solutions at binding to either of the two sites. In analysis of HOTSM, the distinction between a primary site and a modulator site is obtained by choosing different intrinsic affinities and efficacies. For example with 1) $a > 1 > b$ or 2) $a > b > 1$ and $A_S > A_M$, the right side of the receptor, Fig 1, is a primary binding site while the left side is an allosteric site in the classic sense, see earlier section on *Constant a as intrinsic efficacy at the orthosteric site*.

Comparison of HOTSM with ATSM

The constants L , A_S , and a in HOTSM, Fig 1, have the same significance as they have for the ATSM [34]. In the HOTSM, the modulator association constant A_M is the equilibrium affinity constant for the binding of ligand S to a modulator site indicated at a position to the left of R, b is the intrinsic efficacy for ligand S, when bound to the modulator site, and c is the co-operative coefficient for ligand S, when binding to either the primary or the modulator sites on R, Fig 1. Meanwhile, in the ATSM, constants A_M , b , and c are for the association of a heterotropic allosteric molecule, M, to the modulator site. Furthermore, in HOTSM, constant d is a complex constant for the ligand S. Either, it is related to co-operative effects of S, when one binding site is occupied by S, the receptor is activated, and a second ligand S is to be bound either to the primary or the allosteric site. Or, d is related to activation of the receptor when both sites are occupied by S. Constant d has the same significance in the ATSM, but with an M ligand bound at the modulator site. The conclusions in Tables 1 and 2 for the functional-HOTSM are true for the functional-ATSM as well, when replacing ligand S at the modulator site with a heterotropic modulator M and employing fixed concentration ratios of agonist and heterotropic modulator molecules, that is, the concentration ratio $[S]/[M]$ is maintained as the doses of the ligands varies. The theoretical switch from an ATSM analysis, with separate changes in agonist and modulator concentrations, to a HOTSM protocol, with an $[S]/[M]$ ratio fixed as the ligand concentration varies, is illustrated in the 3-D plots of Figs 3 and 4. Keeping $[S]/[M]$ ratios fixed in dose-response experiments is thus equal to following the arrows depicted in the concentration plane of panel B in Figs 3 and 4. An analysis of such protocols is strongly recommended as its outcome may have clinical relevance, see the section below on optimal-fixed-concentration ratios, OFCORs.

For both HOTSM and ATSM, it is the L constant that determines the level of spontaneous activity, Figs 2 and 8. Var-

ying L will essentially lift or decrease the level of spontaneous response before adding any ligands. The L constant was mostly kept at a low value in this analysis. But of course, if experimenting with receptive units that are spontaneously active at a high level, the HOTSM as well as the ATSM with larger values for L will be interesting choices to use in analyses for the behavior of inverse agonists, Fig 2 panel B and D.

As mentioned, c does not affect the third plateau of the HOTSM. For the ATSM, this conclusion is also reached by Hall for his γ constant [34], comparable to the present c coefficient.

HOTSM, ATSM, and inverse agonism

In the cyclic-two-state model, c TSM, discussed in section 2 of the appendix, inverse agonists are defined as ligands that have an intrinsic efficacy parameter a less than 1, when interacting with the primary binding site [55]. Since both HOTSM and ATSM include the c TSM, inverse agonism is also part of these two models. Thus, with a single ligand present, operating at the primary binding site of the ATSM, it will reduce spontaneous activity of the receptive unit if the intrinsic efficacy parameter a is less than unity. For the HOTSM it is a bit more complex, as a single ligand can interact with two binding sites. Conditions for a reduction of spontaneous activity in the HOTSM is when the second plateau is lower than the first plateau or when the first and second plateaus are equal and the third plateau is lower.

Meanwhile, when a heterotropic ligand, that is known to interact with a non-primary binding site, reduces the receptor response, such a reduction in spontaneous activity may be referred to as "inverse allosteric agonism". An experimental parallel to this inverse allosteric agonism is seen for heterotropic ligands of the subfamily 3 of 7-TM receptors including the metabotropic glutamate receptors, mGluRs. Here molecules such as MPEP, Bay36-7620, and CPCCOEt, known to interact with non-primary modifier sites, are presently being marketed as inverse agonists [6]. In accepting the concepts developed for both the c TSM, the HOTSM, and the ATSM, a better term for this type of antagonists, seems to be "inverse allosteric agonists" or just "allosteric modulators". They do not interact directly with the primary glutamate sites.

A point to observe in this connection, is that the above concept of an inverse agonist is at variance with the original use of the term "inverse agonist". The term was introduced for heterotropic inhibitors at the benzodiazepine modulator site of GABA_A ligand-gated channels [46] and actually is still in use with that meaning for allosteric modulators at the GABA_A receptor [2].

HOTSM and optimal-fixed-concentration ratios, OFCORs

For systems that desensitize and display auto-antagonism, it seems relevant to evaluate the effects of a competitive inhibitor included together with agonist application, since competitive antagonists may protect against adverse effects of high agonist concentration, including auto-antagonism.

One such type of analysis was carried out for exocrine secretory processes in a tracheal tissue with acetylcholine as primary ligand and atropine as competitive antagonist [18]. Both drugs seem to operate at an orthosteric and an allosteric binding site. At high enough concentrations, ACh auto-antagonized 100% its own induced secretion, Fig 9A. This auto-antagonism of ACh could be reversed by atropine. Using a single-state reaction scheme with nine receptor conformations and an analysis of the involved equilibrium parameters, it was possible to predict a fixed concentration ratio for a mixture of acetylcholine and atropine, the optimal-fixed-concentration ratio = OFCOR, that would allow maximal stimulation over a large dose range, rather independent of the absolute level of drug concentration. Moreover, an experimental verification of the derived OFCOR was also demonstrated for this system, thus largely avoiding auto-antagonism by ACh as the dose was increased of the ACh/atropine mixture with the right OFCOR [18]. Since there might be potential therapeutic aspects in obtaining OFCORs for clinically relevant situations [25], it seems reasonable to analyze, somehow even on an individual basis, drug desensitization and auto-antagonism responses in the light of HOTSM and ATSM and obtain OFCORs for better drug application. Arguments have also been advocated to circumvent adverse effects and non-specific activities of ligands in regular drug applications by use of allosteric compounds for 7-TM receptors in clinical trials [3,5,30,34,41,47].

Conclusions

The mechanistic, homotropic two-state model, HOTSM, for dose-responses is based on a receptor system with two separate binding sites, one primary (orthosteric) and another modulatory (allosteric), plus a receptive unit that can isomerize between two states, an active and a reactive conformation. HOTSM turns out as a relevant tool to analyze the phenomena of negative co-operativity, auto-antagonism, "concentration-dependent desensitization", or bell-shaped dose-response curves, as well as a model for positive co-operativity or terraced dose-response relationships. The HOTSM can also be fitted to experimentally observed inverse agonism and even reverse terraced and reverse bell-shaped dose-responses with single ligands.

The HOTSM together with cognate forms of the model, such as ATSM, will be of use in the analyses of complex

dose-response data including auto-antagonism and auto-antagonism reversed by modulators as demonstrated by the OFCOR principle. Combining the HOTSM and the ATSM may thus be of help in constructing better drug therapy by mixtures of opposing drugs.

Methods

Data generation and data analyses

SigmaPlot, SP, software version 5.0 (SPSS Science, Chicago, IL) was used both for theoretical data generation and non-linear fitting of theory to experimental data. A user-defined SP program developed by Dr. T'fadalou for generation of all dose-response data is available at <http://www.mfi.ku.dk/bindslev>. Generated dose-response data may be plotted in 2-D for one or two ligands and in 3-D for two ligands. As the 3-D mesh command in the original software only yields symmetrical solutions, a subroutine is included in the developed program for non-symmetrical 3-D mesh plots such as in Figs 3B and 4B.

Appendix. Development of the HOTSM

Here is a brief account of the development of 1) auto-antagonism, 2) the cyclic-two-state model, cTSM, and 3) the ternary-complex model, TCM, leading to the HOTSM.

Single-state models and formulation of auto-antagonism

In biology, a mathematical expression for drug self-inhibition goes back to Haldane's formulation of inhibition at high substrate concentrations with bell-shaped dose-response curves. Haldane's expression for substrate-inhibition was published in his book "Enzymes" [48] and writes in the terminology of the present text:

$$\frac{\text{bound}}{\text{total}} = \frac{S}{\frac{1}{A_S} + S + A_M \cdot S^2}$$

This formula was tested already in its publication year by Murray, who found that the expression simulated experimentally obtained dose-response data [49].

For the next 20 years there was a growing awareness of bell-shaped auto-antagonism in mathematical terms [50]. Single-state theories about self-inhibition were further developed with Ariens' understanding of auto-antagonism from the start of the 1950s, based on experimental observations of dualistic action by single ligands [51]. And, single-state receptor models are still invoked for bell-shaped dose-responses [52,53].

The cyclic two-state model, cTSM

The first explicitly formulated two-state model with complete thermodynamical reciprocity is reaction scheme 5 by Katz and Thesleff [[54], K&T-5] for the desensitizing reaction of muscle contraction measured as membrane poten-

tial under ionophoretic application of acetylcholine at superficial neuro-muscular junctions of frog sartorius muscle. Transcribing the K&T-5 nomenclature into the present terminology, the following K&T-expression is obtained for the concentration-dependent fractional decay

$$\frac{\text{decay}}{\text{total}} = \frac{1}{1 + \frac{1 + A_S \cdot S}{L \cdot (1 + a \cdot A_S \cdot S)}}$$

When this fractional decay is replaced by activation, its formula describes just as well a fractional activity of receptors dependent on ligand concentration. We may call this activation scheme the cyclic two-state model, cTSM. The behavior of cTSM involves spontaneous activity and inverse agonism and was scrutinized in detail by Leff [55].

In the field of enzymology, several approaches were taken in the 1950s to formulate an isomerization step for activation of the "unbound" enzyme moiety [56,57]. Meanwhile, Botts and Drain, as the first, formulated and evaluated a cyclic two-state reaction scheme for substrate to product conversion, involving a reversible conformational change of an enzyme in the un-liganded state [58] parallel to the cTSM for auto-modulation. Homotropic allostery involving two-state receptive units has been en vogue since 1965, exemplified as concerted and sequential models for binding of O₂ to hemoglobin and for substrate-induced enzyme activity with Hill coefficients deviating from unity [7,59]. Cyclic and even cubic two-state models for 7-TM receptors were developed somewhat later [60]. Two-state models for auto-antagonism in monomeric receptive entities have been discussed, of which some are equilibrium models, while others include slow non-equilibrium pathways [27,61].

The ternary-complex model, TCM

The development of ternary-complex models was driven by the discovery of GTP-regulated functions of the adenylyl cyclase enzyme. The GTP-dependence of hormone-activated cAMP production initially discovered by Rodbell and co-workers [62] and the ensuing isolation of the first G protein [63] invoked the whole field of G protein-coupled receptors. During these ten years from 1971 to 1981, the idea was born of a transducing mechanism involving additional membrane-confined components besides the hormone, the receptor, and the effector enzyme and this concept affected signal-transduction models developed during that period [60]. De Lean and co-workers [64] published a survey of such models, now often regarded as *the* reference to the description of the tripartite complexation of receptor, agonist/hormone, and G protein, the ternary-complex model = TCM.

After an unequivocal demonstration of spontaneously active forms of un-liganded 7-TM receptors of the δ opioid sub-family [65], it was natural to combine the cTSM and the TCM in an extended-ternary-complex model, ETCM [66]. The development of a TCM, comprising spontaneous receptor activity, peaked in 1996 with three papers on a cubic ternary-complex model, CTCM [35-37,67]. The culmination of combining a cTSM with a TCM to form a cubic ternary-complex model is a major step forward in analysis of dose-response relations involving G proteins. However, both the HOTSM and the ATSM are alternative themes on cubic two-state models.

Abbreviations

FP, SP and TP = first, second, and third plateau; ATSM = allosteric two-state model; CTCM = cubic ternary-complex model; cTSM = cyclic two-state model; ETCM = extended ternary-complex model; HOTSM = homotropic two-state model; K&T-5 = Katz and Thesleff model 5; OFCOR(s) = optimal-fixed-concentration-ratio(s).

Acknowledgements

E.J. Ariens, 1918 – 2002, contributed significantly to our understanding of auto-antagonism.

References

- Changeux JP: **Allosteric proteins: from regulatory enzymes to receptors – personal recollections.** *Bioessays* 1993, **15**:625-634.
- Maksay G, Thompson SA, Wafford KA: **Allosteric modulators affect the efficacy of partial agonists for recombinant GABA(A) receptors.** *Br J Pharmacol* 2000, **129**:1794-1800.
- Leppik RA, Mynett A, Lazareno S, Birdsall NJ: **Allosteric interactions between the antagonist prazosin and amiloride analogs at the human alpha(1A)-adrenergic receptor.** *Mol Pharmacol* 2000, **57**:436-445.
- Helmstaedt K, Krappmann S, Braus GH: **Allosteric regulation of catalytic activity: Escherichia coli aspartate transcarbamoylase versus yeast chorismate mutase.** *Microbiol Mol Biol Rev* 2001, **65**:404-421.
- Christopoulos A, Kenakin T: **G protein-coupled receptor allostery and complexing.** *Pharmacol Rev* 2002, **54**:323-374.
- Gasparini F, Kuhn R, Pin JP: **Allosteric modulators of group I metabotropic glutamate receptors: novel subtype-selective ligands and therapeutic perspectives.** *Curr Opin Pharmacol* 2002, **2**:43-49.
- Monod J, Wyman J, Changeux J-P: **On the nature of allosteric transitions: A plausible model.** *J Mol Biol* 1965, **12**:88-118.
- Ricard J, Cornish-Bowden A: **Co-operative and allosteric enzymes: 20 years on.** *Eur J Biochem* 1987, **166**:255-272.
- Gamage NU, Duggleby RG, Barnett AC, Tresillian M, Latham CF, Liyou NE, McManus ME, Martin JL: **Structure of a human carcinogen-converting enzyme, SULT1A1. Structural and kinetic implications of substrate inhibition.** *J Biol Chem* 2003, **278**:7655-7662.
- He YA, Roussel F, Halpert JR: **Analysis of homotropic and heterotropic cooperativity of diazepam oxidation by CYP3A4 using site-directed mutagenesis and kinetic modeling.** *Arch Biochem Biophys* 2003, **409**:92-101.
- Arias HR: **Agonist self-inhibitory binding site of the nicotinic acetylcholine receptor.** *J Neurosci Res* 1996, **44**:97-105.
- Lombardi G, Dianzani C, Miglio G, Canonico PL, Fantozzi R: **Characterization of ionotropic glutamate receptors in human lymphocytes.** *Br J Pharmacol* 2001, **133**:936-944.
- Borst P, Elferink RO: **Mammalian ABC transporters in health and disease.** *Annu Rev Biochem* 2002, **71**:537-592.
- Incerpi S, D'Arezzo S, Marino M, Musanti R, Pallottini V, Pascolini A, Trentalancia A: **Short-term activation by low 17beta-estradiol concentrations of the Na+/H+ exchanger in rat aortic smooth muscle cells: physiopathological implications.** *Endocrinology* 2003, **144**:4315-4324.
- Henry ER, Bettati S, Hofrichter J, Eaton WA: **A tertiary two-state allosteric model for hemoglobin.** *Biophys Chem* 2002, **98**:149-164.
- Leiser J, Conn PM, Blum JJ: **Interpretation of dose-response curves for luteinizing hormone release by gonadotropin-releasing hormone, related peptides, and leukotriene C4 according to a hormone/receptor/effector model.** *Proc Natl Acad Sci U S A* 1986, **83**:5963-7.
- Schlessinger J: **Signal transduction by allosteric receptor oligomerization.** *Trends Biochem Sci* 1988, **13**:443-447.
- Winding B, Bindslev N: **Desensitization and reactivation of ACh-regulated exocrine secretion in hen tracheal epithelium.** *Am J Physiol* 1993, **264**:C342-C351.
- Chidiac P, Nouet S, Bouvier M: **Agonist-induced modulation of inverse agonist efficacy at the beta 2-adrenergic receptor.** *Mol Pharmacol* 1996, **50**:662-669.
- Bronnikov GE, Zhang SJ, Cannon B, Nedergaard J: **A dual component analysis explains the distinctive kinetics of cAMP accumulation in brown adipocytes.** *J Biol Chem* 1999, **274**:37770-37780.
- Cuthbert AW: **Benzoquinolines and chloride secretion in murine colonic epithelium.** *Br J Pharmacol* 2003, **138**:1528-1534.
- Hornigold DC, Mistry R, Raymond PD, Blank JL, Challiss RA: **Evidence for cross-talk between M2 and M3 muscarinic acetylcholine receptors in the regulation of second messenger and extracellular signal-regulated kinase signalling pathways in Chinese hamster ovary cells.** *Br J Pharmacol* 2003, **138**:1340-1350.
- Griffin MT, Hsu JC, Shehna D, Ehlert FJ: **Comparison of the pharmacological antagonism of M2 and M3 muscarinic receptors expressed in isolation and in combination.** *Biochem Pharmacol* 2003, **65**:1227-1241.
- Fuh G, Cunningham BC, Fukunaga R, Nagata S, Goeddel DV, Wells JA: **Rational design of potent antagonists to the human growth hormone receptor.** *Science* 1992, **256**:1677-80.
- Talmadge JE: **Pharmacodynamic aspects of peptide administration biological response modifiers.** *Adv Drug Deliv Rev* 1998, **33**:241-252.
- Kühl PW: **Excess-substrate inhibition in enzymology and high-dose inhibition in pharmacology: a reinterpretation [corrected].** *Biochem J* 1994, **298**:171-180.
- Kaiser PM: **Substrate inhibition as a problem of non-linear steady state kinetics with monomeric enzymes.** *J Mol Catal* 1980, **8**:431-442.
- De Meyts P, Urso B, Christoffersen CT, Shymko RM: **Mechanism of insulin and IGF-I receptor activation and signal transduction specificity. Receptor dimer cross-linking, bell-shaped curves, and sustained versus transient signaling.** *Ann N Y Acad Sci* 1995, **766**:388-401.
- Metzger H: **Molecular versatility of antibodies.** *Immunol Rev* 2002, **185**:186-205.
- Rios CD, Jordan BA, Gomes I, Devi LA: **G-protein-coupled receptor dimerization: modulation of receptor function.** *Pharmacol Ther* 2001, **92**:71-87.
- Proška J, Tuček S: **Competition between positive and negative allosteric effectors on muscarinic receptors.** *Mol Pharmacol* 1995, **48**:696-702.
- Ellis J: **Allosteric binding sites on muscarinic receptors.** *Drug Dev Res* 1997, **40**:193-204.
- Zelcer N, Huisman MT, Reid G, Wielinga PR, Breedveld P, Kuil A, Knipscheer P, Schellens JH, Schinkel AH, Borst P: **Evidence for two interacting ligand-binding sites in human MRP2 (ABCC2).** *J Biol Chem* 2003, **278**:23538-23544.
- Hall DA: **Modeling the functional effects of allosteric modulators at pharmacological receptors: an extension of the two-state model of receptor activation.** *Mol Pharmacol* 2000, **58**:1412-1423.
- Weiss JM, Morgan PH, Lutz MW, Kenakin TP: **The Cubic Ternary Complex Receptor–Occupancy Model I. Model Description.** *J Theor Biol* 1996, **178**:151-167.
- Weiss JM, Morgan PH, Lutz MW, Kenakin TP: **The Cubic Ternary Complex Receptor–Occupancy Model II. Understanding Apparent Affinity.** *J Theor Biol* 1996, **178**:169-182.

37. Weiss JM, Morgan PH, Lutz MW, Kenakin TP: **The cubic ternary complex receptor-occupancy model. III. Resurrecting efficacy.** *J Theor Biol* 1996, **181**:381-397.
38. Kinet S, Bernichtein S, Kelly PA, Martial JA, Goffin V: **Biological properties of human prolactin analogs depend not only on global hormone affinity, but also on the relative affinities of both receptor binding sites.** *J Biol Chem* 1999, **274**:26033-26043.
39. Accomazzo MR, Cattaneo S, Nicosia S, Rovati GE: **Bell-shaped curves for prostaglandin-induced modulation of adenylate cyclase: two mutually opposing effects.** *Eur J Pharmacol* 2002, **454**:107-114.
40. Wreggett KA, Wells JW: **Cooperativity manifest in the binding properties of purified cardiac muscarinic receptors.** *J Biol Chem* 1995, **270**:22488-22499.
41. Avlani V, May LT, Sexton PM, Christopoulos A: **Application of a kinetic model to the apparently complex behavior of negative and positive allosteric modulators of muscarinic acetylcholine receptors.** *J Pharmacol Exp Ther* 2004, **308**:1062-72.
42. Zeng F, Wess J: **Molecular aspects of muscarinic receptor dimerization.** *Neuropsychopharmacology* 2000, **23**:S19-31.
43. Migeon JC, Nathanson NM: **Differential regulation of cAMP-mediated gene transcription by m1 and m4 muscarinic acetylcholine receptors. Preferential coupling of m4 receptors to Gi alpha-2.** *J Biol Chem* 1994, **269**:9767-9773.
44. Goffin V, Binart N, Touraine P, Kelly PA: **Prolactin: the new biology of an old hormone.** *Annu Rev Physiol* 2002, **64**:47-67.
45. Colquhoun D: **Binding, gating, affinity and efficacy: the interpretation of structure-activity relationships for agonists and of the effects of mutating receptors.** *Br J Pharmacol* 1998, **125**:924-947.
46. Polc P, Bonetti EP, Schaffner R, Haefely W: **A three-state model of the benzodiazepine receptor explains the interactions between the benzodiazepine antagonist Ro 15-1788, benzodiazepine tranquilizers, beta-carbolines, and phenobarbitone.** *Naunyn - Schmiedebergs Arch Pharmacol* 1982, **321**:260-264.
47. Rees S, Morrow D, Kenakin T: **GPCR drug discovery through the exploitation of allosteric drug binding sites.** *Receptors Channels* 2002, **8**:261-268.
48. Haldane JBS: *Enzymes* London: Longmans, Green & Co; 1930:84-85.
49. Murray DRP: **The inhibition of esterases by excess substrate.** *Biochem J* 1930, **24**:1890-96.
50. Laidler KJ, Hoare JP: **The molecular kinetics of the urea-urease system. I. The kinetic laws.** *J Am Chem Soc* 1949, **71**:2699-2702.
51. Ariens EJ, Simonis AM, De Groot WM: **Affinity and intrinsic-activity in the theory of competitive- and non-competitive inhibition and an analysis of some forms of dualism in action.** *Arch int pharmacodyn* 1955, **100**:298-322.
52. Sakolsky DJ, Ashby B: **Patterns of cyclic AMP formation by coexpressed D1 and D2L dopamine receptors in HEK 293 cells.** *Receptors Channels* 2001, **7**:479-489.
53. Galetin A, Clarke SE, Houston JB: **Quinidine and haloperidol as modifiers of CYP3A4 activity: multisite kinetic model approach.** *Drug Metab Dispos* 2002, **30**:1512-1522.
54. Katz B, Thesleff S: **A study of the 'desensitization' produced by acetylcholine at the motor end-plate.** *J Physiol* 1957, **138**:63-80.
55. Leff P: **The two-state model of receptor activation.** *Trends Pharmacol Sci* 1995, **16**:89-97.
56. Watanabe S, Tomomura Y, Shiokawa H: **Mechanism of muscular contraction. II. Kinetic studies on muscle ATP-ase.** *J Biochem* 1953, **40**:387-402.
57. Blum JJ: **The enzymatic interaction between myosin and nucleotides.** *Arch Biochem Biophys* 1955, **55**:486-511.
58. Botts J, Drain GF: **An illustration of a kinetic analysis: The myosin B-ATP-EDTA system.** In *Conference on the chemistry of muscular contraction 1957* Edited by: The committee of muscle chemistry of Japan. Tokyo: Igaku Shoin; 1958:33-41.
59. Koshland DE Jr, Nemethy G, Filmer D: **Comparison of experimental binding data and theoretical models in proteins containing subunits.** *Biochemistry* 1966, **5**:365-385.
60. De Haën C: **The non-stoichiometric floating receptor model for hormone sensitive adenyl cyclase.** *J Theor Biol* 1976, **58**:383-400.
61. Paton WDM: **A theory of drug action based on the rate of drug-receptor combination.** *Proc Roy Soc Lond* 1961, **154**:21-69.
62. Rodbell M, Krans HM, Pohl SL, Birnbaumer L: **The glucagon-sensitive adenyl cyclase system in plasma membranes of rat liver. IV. Effects of guanyl nucleotides on binding of ¹²⁵I-glucagon.** *J Biol Chem* 1971, **246**:1872-1876.
63. Sternweis PC, Northup JK, Smigel MD, Gilman AG: **The regulatory component of adenylate cyclase. Purification and properties.** *J Biol Chem* 1981, **256**:11517-11526.
64. De Lean A, Stadel JM, Lefkowitz RJ: **A ternary complex model explains the agonist-specific binding properties of the adenylate cyclase-coupled beta-adrenergic receptor.** *J Biol Chem* 1980, **255**:7108-7117.
65. Costa T, Herz A: **Antagonists with negative intrinsic activity at delta opioid receptors coupled to GTP-binding proteins.** *Proc Natl Acad Sci* 1989, **86**:7321-7325.
66. Samama P, Cotecchia S, Costa T, Lefkowitz RJ: **A mutation-induced activated state of the beta 2-adrenergic receptor. Extending the ternary complex model.** *J Biol Chem* 1993, **268**:4625-4636.
67. Kenakin T, Morgan P, Lutz M, Weiss J: **The evolution of drug-receptor models: The cubic ternary complex model for G protein-coupled receptors.** In *The pharmacology of functional, biochemical, and recombinant receptor systems* Edited by: Kenakin T, Angus JA. Berlin: Springer Verlag; 2000:147-165.

Publish with **BioMed Central** and every scientist can read your work free of charge

"BioMed Central will be the most significant development for disseminating the results of biomedical research in our lifetime."

Sir Paul Nurse, Cancer Research UK

Your research papers will be:

- available free of charge to the entire biomedical community
- peer reviewed and published immediately upon acceptance
- cited in PubMed and archived on PubMed Central
- yours — you keep the copyright

Submit your manuscript here:
http://www.biomedcentral.com/info/publishing_adv.asp

